Pergamon

Geochimica et Cosmochimica Acta, Vol. 64, No. 11, pp. 1925–1944, 2000

0016-7037/00 $20.00 + .00

PII S0016-7037(00)00342-2

Helium isotopes, tectonics and heat flow in the Northern Caucasus

B. G. POLYAK,[1,*] I. N. TOLSTIKHIN,[2] I. L. KAMENSKY,[2] L. E. YAKOVLEV,[1] B. MARTY,[3] and A. L. CHESHKO[1]

[1]Geological Institute, Academy of Sciences, Moscow, 109017 Russia
[2]Geological Institute, Academy of Sciences Kola Branch, Apatity, 184200 Russia
[3] CNRS - CRPG B.P. 20, 54501 Vandoeuvre-Nancy Cedex, Nancy, France

(*Received September* 25, 1998; *accepted in revised form February* 2, 2000)

Abstract—109 new measurements of $^3He/^4He \equiv R$ in subsurface fluids of the Northern Caucasus coupled with the data obtained previously allow regional regularities in the distribution of helium isotopic composition to be examined. Cis-Caucasian foredeeps show the lowest radiogenic *R*-values. The average R_{av}-value is slightly higher in gases of the Scythian plate beyond the Stavropol arch. Within the arch, elevated $R = (1.6–4.5) \times 10^{-7}$ indicates an input of mantle-derived helium. This input is even more evident to the south of Starvropol arch, in the Caucasian Mineral Water area, where the ≈8 Ma old laccolithes occur and *R*-values approach $(5–11) \times 10^{-7}$. The highest *R*-values, up to $(0.7–0.9) \times 10^{-5}$, are observed further to the south, in the central segment of the Greater Caucasus, where recent volcanism is manifested. Enhanced *R*-values do not correlate with the crustal thickness but reflect degassing of magmatic reservoirs including those yet unknown.

According to the recent Sr-Nd-O data, the young volcanic rocks are of mantle affinity but they are contaminated by a crustal component. The average R_{av}-values in fluids and $^{87}Sr/^{86}Sr$ ratios in host magmatic rocks show an inverse correlation suggesting mixing of crustal and mantle materials. *R*-values vary inversely with apatite fission-track ages of crystalline basement rocks. The ages increase westward of the Elbrus volcano, most likely recording the thermal degradation of the Greater Caucasus since the pre-Cainozoic magmatic activity. A direct correlation between R_{av}-values and *background* conductive heat flow densities implies that discharge of the mantle melts into the crust is the common cause of the geochemical, geochronological and geothermal regularities observed.

Elevated *R*-values are generally observed in CO_2-bearing fluids, low values are typical of CH_4 gases, a few N_2-rich gases display highly variable *R*. Relationships between the major gas constituents and noble gas isotopes are discussed. Fractionation, loss, and gain of these species are considered as the processes controlling the compositions of underground fluids. *Copyright © 2000 Elsevier Science Ltd*

1. INTRODUCTION

$^3He/^4He = R$ ratios in underground fluids of the Alpine-Himalayan folding belt were first investigated in the Caucasus by Matveeva et al. (1978) who reported a highly variable *R* from 3.1×10^{-8}, corresponding to radiogenic helium generated within terrestrial rocks, to $\approx 0.9 \times 10^{-5}$ indicating a dominant contribution of mantle-derived helium with $^3He/^4He = R \sim 10^{-5}$. Additionally, some regularity in the lateral distribution of *R*-values was perceived for the Caucasus region. The enhanced *R*-values appear to be typical of fluids in the Transcaucasian transversal uplift zone that crosses the Greater Caucasus meganticlinorium through its central part, where manifestations of Neogene-Quaternary volcanism has occurred. Matveeva et al. (1978) reported *R*-values uncorrected for air contamination because of lack of parallel measurements of Ne and/or Ar isotope abundances. Later Gazaliev and Prasolov (1988), Prasolov (1990), and Lavrushin et al. (1996) presented additional *R*-measurements.

High *R*, up to 0.9×10^{-5}, were also reported for fluids from the Apennine segment of the Alpine belt (Polyak et al., 1979b). These authors revealed a He-Sr isotope correlation reflecting crust-mantle interaction during N-Q volcanism in the Apennines. Results presented by Polyak et al. (1979b) were corroborated by Hooker et al. (1985) who studied, among others, the Larderello geothermal field supplementing earlier measurements reported by Nuti (1984). Helium isotope abundances in Italian fluids were discussed later by Sano et al. (1989), Tedesco et al. (1990) Tedesco et al. (1998), Marty et al. (1992) Marty et al. (1994), Elliot et al. (1993), Tedesco (1996), Tedesco and Nagao (1996), and Allard et al. (1997).

A contribution of mantle-derived helium was observed in fluids from many other fragments of the Alpine orogenic belt where the Cainozoic magmatic activity occurred: Greece (Oxburgh et al., 1987), Turkey (Hill et al., 1986; Kipfer, 1991), and others. On the contrary, in the Alps themselves underground fluids usually contain He with low *R* from $\approx 3 \times 10^{-8}$ to $\approx 15 \times 10^{-8}$ (Marty et al., 1992). Studies of the Cis-Alpine Molasse foredeep (Loosli et al., 1995; Tolstikhin et al., 1996) showed that such a range could result from the radiogenic helium production by host rocks. *R* increases up to 8.4×10^{-7} in one site of Southern Austria and to $(5.3–8.4) \times 10^{-6}$ in two sites on the border with the Pannonian basin (Marty et al., 1992). These authors considered a large thickness of the earth crust and weak magmatic activity as the reasons for the low *R*-values in the Alps, while rare enhanced values in the Eastern Alps could be related to N-Q volcanism within the Pannonian basin. Low Alpine-like $R < 2 \times 10^{-7}$ are also typical for the Himalayan segment of the belt (Craig and Craig, 1983; Giggenbach et al., 1983; Zuhuang et al., 1986), and Yokoyama et al. (1999) have measured slightly higher $R = (16.8–30.8) \times 10^{-8}$ in spring gases from the southern Tibet.

The Pannonian basin is considered as one of the largest

*Author to whom correspondence should be addressed (polyak@geo.tv-sign.ru).

regional positive geothermal anomalies in Europe. Here, as in the adjacent Wienna Basin, helium isotopes in underground fluids were thoroughly studied with an emphasis on the deciphering of hydrologic regime (Nagao, 1979; Cornides et al., 1986; Deak et al., 1989; Martell et al., 1989; Ballentine et al., 1991; Ballentine and O'Nions, 1993; Ballentine and O'Nions, 1994; O'Nions and Ballentine, 1993; Stute et al., 1992). R varies usually from 4×10^{-7} to 7×10^{-7} but locally can be as high as to 5.5×10^{-6}, indicating a substantial contribution of mantle-derived helium.

The earth mantle is considered as the principal ^{3}He reservoir in all contributions referred above. However the flux of extraterrestrial helium, carried by interplanetary dust particles (IDP), also supplies ^{3}He to terrestrial sediments at about constant rate $\sim 1 \times 10^{-12}$ cc STP cm^{-2} ka^{-1} (Merrihue, 1964; Farley, 1995; Marcantonio et al., 1998). After IDPs have reached sediments, the evolution of helium isotopic composition depends on the sedimentation rates, the U and Th concentrations, the rates of loss of helium isotopes, and the age. Sedimentation rates for areas remote from continents, such as the central Pacific, is of the order of $\sim$0.1 cm ka^{-1}, by a factor of 100 to 10,000 less than those for continental margins or intercontinental seas (e.g., Marcantonio et al., 1998). Because of this great difference, accumulating radiogenic ^{3}He overshadows the extraterrestrial ^{3}He in sediments having U $\approx$ 1–3 ppm , Th/U $\approx$ 4, and age 1 to 100 Ma; sediments filling the Cis-Caucasian foredeeps are within this diapason.

Tolstikhin et al. (1996) and Tolstikhin et al. (1999) suggested and verified another process leading to enhanced ^{3}He/^{4}He ratios in chemical sediments, anhydrite and carbonates: radiogenic helium isotope fractionation related to a specific behaviour of ^{3}H, ^{3}He precursor. However the only example of groundwater, bearing the isotopically fractionated radiogenic He, shows very low He/Ne ratios and ^{3}He/^{4}He $\leq 1.5 \times 10^{-7}$, much less than those in fluids investigated in this contribution.

Therefore we consider the enhanced ^{3}He/^{4}He ratios in a conservative way as those resulting from mixing of crustal radiogenic and mantle partially primordial helium.

This paper examines both published and newly obtained data on He isotope abundances in underground fluids of the Northern Caucasus. A general aim is to refine relationships between R-value (considered as a measure of crust-mantle interaction) and magmatism, heat flow, groundwater circulation, major gas abundances in subsurface fluids, and other isotopic data. Unlike rocks, the fluids naturally integrate R-values, characterise large-scale geological blocks and therefore provide an important step from local to regional characteristics.

2. GEOLOGICAL SETTING

The earth crust of the Northern Caucasus includes blocks formed during Baikalian, Hercynian, Cimmerian, and proper Alpine orogenic cycles (Adamiya et al., 1989). Philip et al. (1989), applying plate tectonic concepts, revised evolution of the Caucasus which is briefly resumed below.

During the Jurassic, Cretaceous and Paleogene, a marginal sea covered the Scythian plate and was bounded in the south by the calc-alkaline volcanic arc, corresponding to the present-day position of the Greater Caucasus. After closing the Tetis Ocean (about 20 Ma), the marginal basin was reduced. The following drift of the Arabian Plate to the north initiated continental collision and uplift of the Greater Caucasus. It began 5 Ma ago and escalated 3.5 Ma ago. "A remainder of the volcanic arc may still be seen to the west of the collision zone, from Kazbek to Elbrus. . . In general, the structures of the Greater Caucasus are overturned towards the south. Nevertheless, thrusting to the north occurs in Daghestan and next to the southern border of the Kuban basin" termed hereafter as the Indol-Kuban foredeep (Philip et al., 1989).

Figure 1 presents tectonic patterns of the Greater Caucasus. In comments to the A-B cross-section, Philip et al. (1989) emphasised that a monocline of the Greater Caucasus northern slope "continues smoothly into the Scythian Plate" and "is formed by a sequence of Mesozoic to Quaternary layers overlying the Palaeozoic basement", whereas the C-D cross-section demonstrates "the asymmetrical Mesozoic to Quaternary Terek basin (Terek-Caspian foredeep) that thickens to the south, with maximum depth of 12 km" and "the Daghestan folded zone, composed of calcareous Mesozoic to Cainozoic sediments, that thrusts to the north over Terek basin. . . . No recent volcanism is observed" in this region (Philip et al., 1989).

Milanovsky and Koronovsky (1973) noticed magmatic reactivation of the Central Caucasus during the Late Miocene when stratovolcanoes and monogenic cones, lava and tufflava plateaux, and hypabyssal intrusions were formed; the latter are mainly unexposed on the earth surface. The manifestations of magmatic and volcanic processes are observed in the Elbrus-Kazbek volcanic province. The earliest of these manifestations were laccolithes of trachyrhyolite situated to the north of Elbrus volcano in the Caucasian Mineral Waters area (CMW). The ^{40}Ar/^{39}Ar ages of these laccolithes range from 8.41 to 7.79 Ma (Pohl et al., 1993). Later the northern boundary of the volcanic manifestations shifted to the south. In general, Elbrus products are calc-alkaline acidic rocks that vary from rhyolites to andesidacites, whereas the volcanic rocks of the Kazbek sector are more basic (from andesidacites to andesites, rarely andesibasalts). Compared to the Elbrus volcanic rocks, the CMW trachyrhyolites contain up to 3 times more K_2O (6.9 wt%) and 2–5 times more Ce, Rb, Sr, Ba, U, Th and Pb indicating a higher degree of crustal contamination (Popov, 1987).

The depth to the Moho discontinuity beneath the Caucasus varies from $<$40 to $>$60 km (Shengelaya, 1978). Within the Elbrus sector the total crustal thickness is rather uniform (45–50 km), whereas that of the granite layer varies from 24 km below the Northern Caucasus to 16 km under the volcano (Milanovsky et al., 1989). According to gravimetric and seismological data, the crustal rock density is reduced within the depth interval from 10 to 20 km beneath the Elbrus. These studies also found a large segment-like lessened-V_p body centred below the Elbrus with a radius $\sim$ 50 km. Garetovskaya et al. (1986) interpreted this body as an "asthenolense". All the above indicates a high magmatic potential for the Greater Caucasus central segment.

3. EXPERIMENTAL

The free gases spontaneously escaping from underground fluids discharged on the earth surface (through natural springs or boreholes) are mainly discussed in this work. Most of the samples were collected in 220 cm^3 glass containers using a simple water replacement technique. Several fluid samples from hydrocarbon fields have been col-

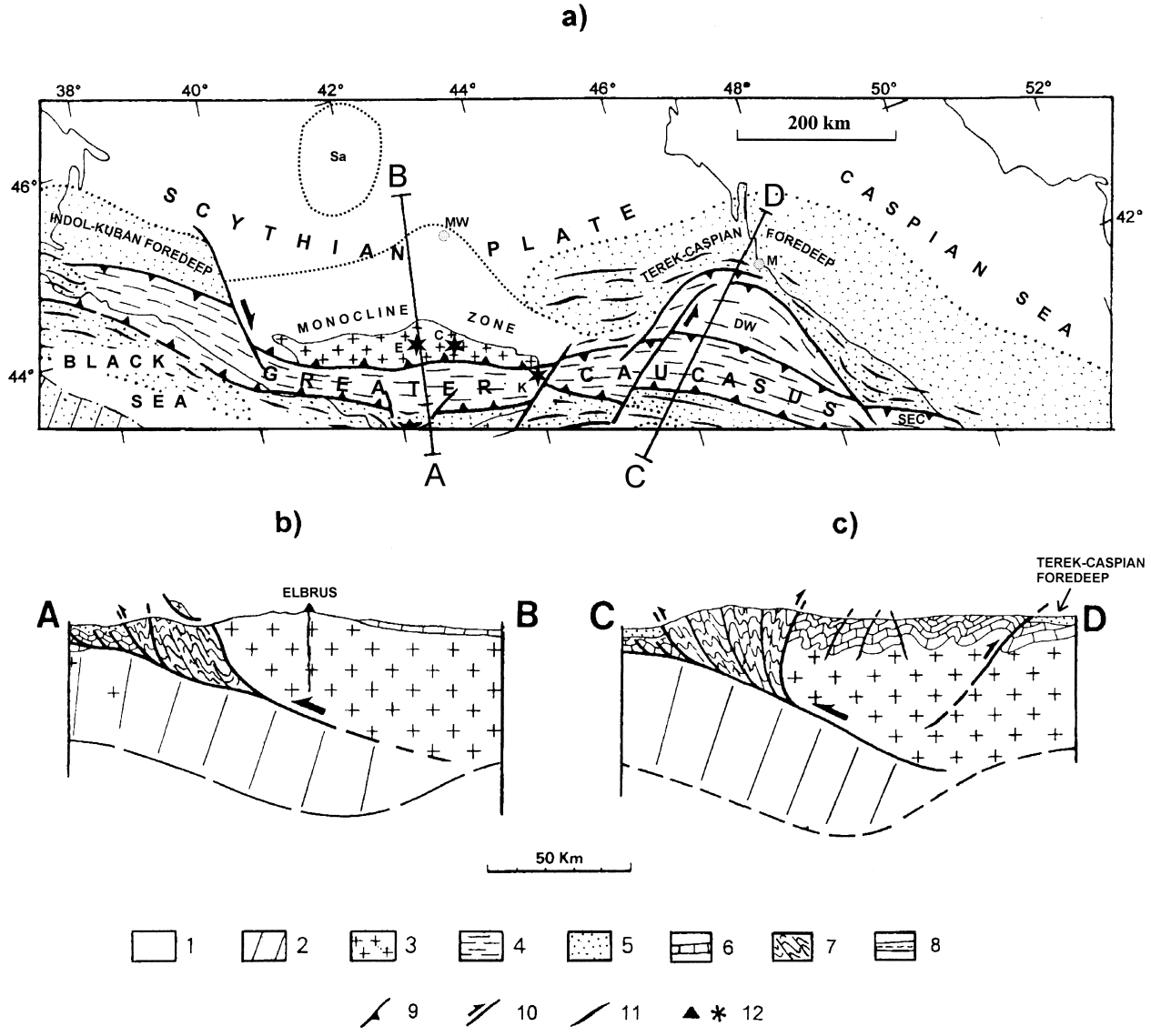

Fig. 1. Tectonic pattern of the Northern Caucasus (a fragment from Philip et al., 1989, modified). (a) structural map (tectonic units renamed in accordance with the CGMW standards), (b) and (c) cross-sections AB and CD, respectively (see map for positions). Legend: (1) continental crust; (2) oceanic or intermediate crust; (3) outcrops of continental basement; (4) folding within Mesozoic to Paleogene sediments; (5) young sedimentary basins (foredeeps); (6) Mesozoic to Paleogene layers; (7) strong deformation of Mesozoic layers; (8) Oligocene to Miocene sediments; (9) major thrust faults; (10) major strike-slip faults; (11) folding within young sedimentary basins (foredeeps); (12) Neogene to Quaternary volcanic centres marked as (E) Elbrus, (C) Chegem, and (K) Kazbek. Other abbreviations denote (Sa) Stavropol arch, (DW) Daghestan wedge (or Daghestan folded zone), and cities (MW) Mineral'nye Wody and (M) Makhachkala.

lected with a special sampler or in steel containers under head pressures (Prasolov, 1990).

He, Ne, and Ar concentrations were determined volumetrically using Khlopin-Gerling glass-mercury device and the purified specimens of (He + Ne) and Ar were sealed in glass ampoules. The dynamic range of device is from 10 to 10^{-5} vol% (from 100000 to 0.1 ppm). Initial portion of gas varied from 3 to 200 cm^3. Blank values are $\leq 10^{-7}$ cc for He and $\leq 10^{-6}$ cc for Ar; the accuracy of measurement of optimal concentrations is $\pm 2\%$ (1σ).

Several (up to 15) ampoules were loaded into high-vacuum ampoule breaker connected with an inlet line to a single-beam mass-spectrometer MI-1201 operating under static mode. Hydrogen multiplet is surpressed by rejuvenated Ti-mirror cooled by liquid nitrogen so that current of HD^+ ions is less than 10^{-17} A.

Sensitivity of the mass-spectrometer for He and Ar is (3–5) $\times$ 10^{-5} A/torr and (3–5) $\times$ 10^{-6}, respectively. The resolution is $\approx$1000, which allows HD-^{3}He duplet to be completely separated. The shape of peak is satisfactory flat (Kamensky et al., 1990). The total blanks of ^{4}He and ^{40}Ar in ampoule breaker, inlet line and mass-spectrometer chamber are 1×10^{-10} and 5×10^{-9} cm^3 STP, respectively.

Computer controls scanning of the magnetic field by a special device and measuring of the ion beams. Reproducibility of isotope analysis (1σ) depending on the measured isotopic ratios is:

25, 10, and 3 % for ^{3}He/^{4}He $\sim 10^{-8}$, $\sim 10^{-7}$, and $\sim 10^{-6}$, respectively;

20, 10, and 3 %, for ^{4}He/^{20}Ne $\sim 10^4$, $\sim 10^2$, and $\sim$1, respectively;

1 and 0.5 %, for ^{40}Ar/^{36}Ar $\sim$ 1000 and $\sim$ 300, respectively.

Tables 1 and 2 comprise new and previous results and Figure 2 shows the location of the sampling points.

4. DATA PROCESSING

Using R in underground fluids for elucidation of lateral R variations should be preceded by an analysis of changeability of this parameter with time and depth.

17 sites within the region under study were sampled repeatedly since 1968. Besides, one borehole was sampled 11 times (Prasolov, 1990). These data (Table 1) show that the temporal R variations are insignificant in all but one case, and a single specimen may be considered as representative of a given locality. The time-diverse R-values from the same locality were averaged. Repeated measurements in Iceland, Italy, Mexico, New Zealand, Kamchatka, Tien Shan, and Baikalia also demonstrate near-constant R in an individual object. The few exceptions were related to active volcanoes.

R measurements at different depths in the same borehole are very rare. However R-values are available for different depths in the boreholes situated within one and the same geological unit (Table 1). These data demonstrate that R variations with depth are statistically insignificant. Therefore, for the mapping of lateral variations, the R-values at different depths within one and the same borehole were averaged as well.

5. RESULTS AND DISCUSSION

5.1. Helium Isotopes and Major Gases

CH_4, N_2, and CO_2 are the major gas components of the fluids (Table 2). Figure 3 shows relationships between these components, helium concentrations and $^3He/^4He$ ratios; two principal terrestrial reservoirs are also shown for comparison. The first is MORB-like-source characterised by $R_{MORB} = (1150 \pm 100) \times 10^{-8}$, $(CO_2/^3He)_{MORB} = (0.9 \pm 0.2) \times 10^9$, and the total helium concentration [He] $\approx$ [^{4}He] $\approx$ $(^3He/CO_2)_{MORB} \times 1/R_{MORB} = 97 \pm 30$ mcc/L (Marty and Tolstikhin, 1998; hereafter mcc/L $= 10^{-3}$ cubic centimetre STP per litre of gas phase = ppm).

The leftward dispersion from the MORB rectangle could originate from: (1) an addition of He-depleted major gas constituent(s) or (2) He loss increasing $CO_2/^3He$ ratio in a gas-water system. The He loss could result from solubility-controlled processes in accord with two scenarios. The first scenario (2.1) envisages partial dissolution of MORB-source gas, which would enhanced $CO_2/^3He$ ratio in the water phase because of a higher solubility of CO_2. Subsequent substantial degassing of this groundwater produces gas with $CO_2/^3He > CO_2/^3He_{MORB}$. This inequality is actually observed in a number of samples from the Greater Caucasus.

The second scenario (2.2) implies a two-stage fractional degassing of groundwater, having initially MORB $CO_2/^3He$ ratio. After the first stage, the residual groundwater would have characterised by higher $CO_2/^3He$ ratios. During the second stage, the gas having similar ratios could be extracted, providing a high enough degree of degassing. Simultaneously a noticeable fractionation of atmospheric noble gases dissolved in groundwaters must occur. This is not observed in our samples: $^{20}Ne/^{36}Ar$ ratios vary between 0.53 (air) and 0.14 (air-saturated water) supporting scenario (2.1).

The rightward dispersion could be caused by fractional degassing leading to preferable transfer of less soluble He in a gas phase or/and by consumption of the major chemically active component.

The second end-member is a crustal helium reservoir with $R \approx (2 \pm 1) \times 10^{-8}$. The slope band represents mixing between the mantle MORB-like reservoir and crustal He.

The experimental data-points in Figure 3 lay mainly to the left off the slope band, within the sector limited by this band and by the horizontal trend to the left of the MORB rectangle. Generally CO_2-rich gases from the Greater Caucasus meganticlinorium show enhanced $CO_2/^3He$ ratios, in some specimens approaching $\sim 10^{12}$ that is $\sim$1000 times above the MORB ratio. As shown above this could originate from contribution of CO_2-rich He-free component as specified under (1) above or/and from the solubility-controlled processes described under (2.1). Carbon isotopic data allow a principal source of CO_2 to be identify. $\delta^{13}C$ values in CO_2-rich gases from the Elbrus vicinity, with the average $-5.9‰$ (Buachidze and Mkheidze, 1989), are within the accepted mantle diapason, $-6 \pm 3‰$ (Trull et al., 1993), implying the mantle source for CO_2.

Irrespective of the major gas constituent, all data available for the Greater Caucasus meganticlinorium (GC) including its south-eastern sector (SEC) and the monocline zone (MZ) excepting the CMW area show an inverse correlation between He-depleted mantle end member and ^{4}He-enriched crustal one (Fig. 3). The inverse R-[He] correlation was also observed previously in several other regions characterised by a young magmatic activity, e.g., in the Trans-Mexican volcanic belt (Polyak et al., 1982), the Rhine graben (Griesshaber et al., 1989), and the Baikal rift (Polyak et al., 1992, Polyak et al., 1994).

CMW gases differ from those in the Greater Caucasus. A narrow range of lower R-values indicates a considerable contribution of crustal helium. [He] varies within almost 3 orders of magnitude, but the concentrations are dominantly above that in MORB. CO_2 is the major component as well, but $CO_2/^3He$ ratios, varying from 3×10^7 to 6×10^{10}, are generally below the MORB value. The simplest explanation of these relationships envisages mixing of the mantle and crustal components along with CO_2-He fractionation.

Mixing of a mantle-derived fluid with a ^{4}He-bearing underground water would lead to decrease of R-value corresponding to the growth of helium concentration. A maximal concentration of crustal helium in the underground water could be estimated from $^4He/^{20}Ne \leq 2000$ (Table 1) and Ne solubility, assuming air-saturated concentration of Ne (the assumption is supported by observed $^{20}Ne/^{36}Ar$ ratios, see above). The estimated water-dissolved [^{4}He] $\leq 4 \times 10^{-4}$ cc STP He per g H_2O appears to be quite reasonable; it is an order of magnitude lower than those observed in many sedimentary basins (Ivanov et al., 1978; Tolstikhin et al., 1996). The mean CMW $R \approx 8 \times 10^{-7}$ indicates [He] increase by a factor of 13, and the corresponding slope track is highlighted in Fig. 3.

CO_2 carbon isotopic compositions is noticeably heavier in CMW gases as compare with the mantle composition: the average $\delta^{13}C = -4.0‰$ (Potapov et al., 1998; Voitov et al., 1993; Voitov et al., 1994; Voitov et al., 1996; Voitov et al., 1998; Zor'kin et al., 1981, and our measurements). This heavier carbon seems to indicate a contribution from marine carbonates available in sedimentary cover of the CMW area. Because $\delta^{13}C$ in the crustal CO_2 component is not known, it is not possible to estimate its contribution. Qualitatively the [^{4}He] decrease caused by CO_2 addition is shown in Figure 3 as the horizontal

Table 1. He, Ne and Ar abundances and isotopic composition in the Northern Caucasus subsurface fluids[a].

No. in Fig. 2	Location N, E	Unit[b]	Name	Year of sample	Depth m	Sample index	He	Ne	Ar	$^3He/^4He, 10^{-8}$		$\frac{^4He}{^{20}Ne}$	$\frac{^{40}Ar}{^{36}Ar}$	Ref.
							mcc/L = ppm			meas.	corr.			
1	46°05, 38°57′	SP	Kanevskaya prosp. area, hole 60	<1978	1700	EMP-6	209			5.7				4
2	46°33, 39°04′	SP	Starominskaya prosp. area, hole 36	<1978	2100	EMP-8	178			8.3				4
3	45°56, 39°17′	SP	Chelbasskaya prosp. area, hole	<1978	2150	EMP-5	164			7				4
4	46°19, 39°24′	SP	Leningradskaya prosp. area, hole 52	<1978	2100	EMP-7	173			8.6				4
5	45°46, 39°32′	SP	Serdyukovskaya prosp. area, hole 37	<1978	2650	EMP-4	153			8.2				4
6	45°23, 39°32′	SP	Berezanskaya prosp. area, hole 1051	<1978	2620	EMP-3	156			11.1				4
7	46°34, 39°39′	SP	Kuschevskaya prosp. area, hole 48	<1978	1380	EMP-9	231			10.4				4
8	45°13, 39°43′	SP	Ust-Labinskaya prosp. area, hole	<1978	3370	EMP-2	113			8				4
9	45°16, 39°51′	SP	Nekrasovskaya prosp. area, hole	<1978	3350	EMP-1	152			7.2				4
10	45°19, 39°58′	SP	Ladozhskaya prosp. area, hole	<1978	936	ESM-14	33			5.5				1
10	45°19, 39°58′	SP	Ladozhskaya prosp. area, hole	<1978	3400	EMP-74b	83			6.8				5
11	44°48, 40°05′	SP	Maykopskaya prosp. area, hole 137	<1978	2558	ESM-16	128			5.4				1
12	44°23, 40°05′	SP	Krasnodagestanskaya prosp. area, hole	<1978	1500	EMP-129d	600			5.1				5
13	44°46, 41°11′	SP	Yuzhno-Sovietskaya prosp. area, hole 32	<1978	2971	ESM-18	80			7.7				1
14	44°33, 41°23′	SP	Besskorbnenskoe prosp. area, hole	<1978	2918	ESM-19	150			8.5				1
15	45°46, 43°40′	SP	Iki-Burulskaya prosp. area, hole	<1978		EMP-105				9.4				5
16	45°14, 43°41′	SP	Mirnenskaya prosp. area, hole	<1978	450	EMP-113a	72		97	4.4				5
17	44°57, 45°09′	SP	Bezvodnenskoe prosp. area, hole 890	<1978	1448	ESM-20	270			8				1
18	44°52, 45°40′	SP	Yubileynaya prosp. area, hole 2	<1978	4432	ESM-21	110			8.6				1
19	44°46, 45°45′	SP	Solonchakovskaya prosp. area, hole 15	<1978	3618	ESM-22	290		68	8				1
20	45°20, 46°13′	SP	Krasno-Kamyshanskaya prosp. area, hole	<1978		EMP-196b				5.8				5
21	45°32, 46°20′	SP	Severo-Kamyshanskaya prosp. area, hole	<1978	2200	EMP-194b	90			8.6				5
22	45°23, 46°33′	SP	Naryn-Khodukskaya prosp. area, hole	<1978	2230	EMP-195c	210			3.7				5
		SP	Novo-Troitskaya prosp. area, hole	<1978		EMP-210′	10		30	16	15		300	3
		SP	Listvinskaya prosp. area, hole	<1978	2200	EMP-263′	184		71	1.4				7
25	45°38, 40°31′	Sa	Mitrofanovskaya prosp. area, hole 4	<1978	3654	ESM-8	120			15.8				1
26	45°32, 40°51′	Sa	Sokolovskaya prosp. area, hole	<1978	3593	ESM-10	135			20				1
27	45°36, 41°04′	Sa	Rasshevatskaya prosp. area, hole 46	<1978	2799	ESM-9	210			33				1
28	45°17, 41°48′	Sa	Sev.-Stavropolskaya prosp. area, hole 80	<1978	952	ESM-11	350			45				1
		IKF	Begol Spr., spring	<1978	0	EMP-8d′	30		90	4.3	4.1		316	3
30	45°09, 36°21′	IKF	Priozernaya prosp. area, hole	<1978		EMP-8b	40		140	4.4	4.2		328	3
31	45°25, 36°28′	IKF	Andrusova m. v. (Bulganak group), spring	1968	0	EMP-91′a	140			5.4				3
31	45°25, 36°28′	IKF	Oldenburgskogo m.v. (Bulganak group), spring	1968	0	EMP-91′b	100		120	6	5.9			3
31	45°25, 36°28′	IKF	Trubetskogo m. v. (Bulganak group), spring	1968	0	EMP-91′c	110		200	3.7	3.7		348	3
31	45°25, 36°28′	IKF	Pavlova Sopka m. v. (Bulganak group), spring	1968	0	EMP-PS	60		190	3.5	3.4		325	3
31	45°25, 36°28′	IKF	Vernadskogo Sopka m. v. (Bulganak group), spring	1968	0	EMP-VS	90		250	3.6	3.5		328	3
32	45°12, 36°46′	IKF	Karabetova gora m.v., spring	1968	0	EMP-93′	30		80	6.2	6		324	3
32	45°12, 36°46′	IKF	Karabetova gora m. v., spring	1990	0	VAI-9	34	1.9	1520	6	3.9	19.7	300	7
33	45°26, 36°55′	IKF	Kuchugurskii m. v., spring	1994	0	VL-1/94	3.05	0.094	77	8.5	7.9	35.8	313	7
34	45°08, 36°56′	IKF	Bugazskii m. v. (Bugaz group), spring	1968	0	EMP-92′a	40		40	5.1	5		381	3
34	45°08, 36°56′	IKF	Yuzhno-Bugazskii m.v. (Bugaz group), spring	1968	0	EMP-92′b	20		80	5.1	4.8		338	3
35	45°17, 36°57′	IKF	Shapurskii m. v., spring	1994	0	VL-17/94	7.7	0.58	415	18.6	16	14.5	298	7
36	45°09, 36°57′	IKF	Polivadina m. v., spring	1994	0	VL-5/94a	16.2	0.12	106	4.6	4.3	153	301	7
36	45°09, 36°57′	IKF	Polivadina m. v., spring	1994	0	VL-5/94b	16.8	0.118	106	3.9	3.6	156	301	7
37	45°19, 37°02′	IKF	Zapadnyi Tsimbali m. v., spring	1990	0	VAI-6	48	0.517	648	4.5	4.1	102	302	7
38	45°19, 37°03′	IKF	Vostochnyi Tsimbali m. v., spring	1990	0	VAI-3	49	0.534	648	5.2	4.8	101	302	7
39	45°19, 37°04′	IKF	Akhtanizovskii m. v., spring	1990	0	VAI-1	103	0.534	567	5.5	5.3	212	310	7
40	45°22, 37°06′	IKF	Sinyaya Balka m. v., spring	1994	0	VL-14/94	30.1	0.15	137	6	5.8	219	314	7

(Continued)

Table 1. Continued

No. in Fig. 2	Location N, E	Unit[b]	Name	Year of sample	Depth m	Sample index	He	Ne	Ar	$^3He/^4He, 10^{-8}$		$\frac{^4He}{^{20}Ne}$	$\frac{^{40}Ar}{^{36}Ar}$	Ref.
							mcc/L = ppm			meas.	corr.			
41	45°17, 37°06′	IKF	Borisa and Gleba m. v., spring	1990	0	VAI-2	114	0.755	691	5.3	5	166	307	7
42	45°20, 37°13′	IKF	Sopka m. v., spring	1994	0	VL-23/94	50.1	0.191	229	4.2	4.1	288.5	321	7
43	45°15, 37°13′	IKF	Severo-Neftyanoi m. v., spring	1994	0	VL-20/94	13.5	0.148	149	4.8	4.4	100.1	304	7
44	45°11, 37°13′	IKF	Yuzhno-Neftyanoi m. v., Centr. spring	1994	0	VL-18/94	8.4	0.1	85.5	4.9	4.5	92.5	303	7
44	45°11, 37°13′	IKF	Yuzhno-Neftyanoi mud v, East. spring	1994	0	VL-19/94	1.8	0.21	212	13.3	9.0	9.2	299	7
45	45°20, 37°17′	IKF	Golubitskii morskoi m. v., spring	1994	0	VL-2/94	13.7	0.1	122	3.1	2.8	150	307	7
46	45°16, 37°24′	IKF	Miska m. v., spring	1990	0	VAI-7	15	0.349	409	5	4.1	47.3	301	7
47	44°54, 37°36′	IKF	Semigorskii y m. v., spring	1968	0	EMP-SS	120		60	6.3	6.3		428	7
47	44°54, 37°36′	IKF	Semigorskii m. v., spring	1994	0	VL-9/94	204	0.14	132	5.3	5.3	1629	342	7
48	45°03, 37°37′	IKF	Shugo m. v., spring 1	1994	0	VI-13/94	22.5	0.09	86.1	4.1	4.0	275	320	7
48	45°03, 37°37′	IKF	Shugo m. v., spring 2	1994	0	VL-13-2/94	35.4	0.41	262	4.2	3.8	94	302	7
49	45°13, 37°38′	IKF	Gnilaya Sopka m. v., spring	1990	0	VAI-GS	12	1.63	1470	14.3	9.5	8.1	299	7
49	45°13, 37°38′	IKF	Gnilaya Sopka m. v., East. spring	1994	0	VL-3/94a	40	0.2	191	3.5	3.3	220	314	7
49	45°13, 37°38′	IKF	Gnilaya Sopka m. v., East. spring	1994	0	VL-3/94b	39	0.24	194	3.5	3.3	182	312	7
50	44°59, 37°44′	IKF	Gladkovskii m. v., spring	1994	0	VL-11/94a	876	0.17	272	4.6	4.8	5700	658	7
50	44°59, 37°44′	IKF	Gladkovskii m. v., spring	1994	0	VL-11/94b	868	0.13	271	5	5.0	7450	670	7
51	45°03, 37°50′	IKF	Kievskii m. v., spring	1994	0	VL-12/94	22	0.16	135	3.4	3.1	151	302	7
52	44°49, 38°30′	IKF	Zybza prosp. area, hole	<1978	1360–2000	EMP-19c	80		75	3.7	3.7		370	3
53	44°09, 39°49′	IKF	Samurskaya prosp. area, hole	<1978	920–1860	EMP-31a	420		65	9.4	9.4		537	3
54	43°21, 44°28′	TCF	Zamankul'skaya prosp. area, hole	<1978	3700	EMP-50	25			4.9				5
55	43°20, 45°09′	TCF	Sernovodsk Spr., spring	1989	0	89BP-1	173		8860	3.3	3.3	26.4	307	7
56	43°22, 45°38′	TCF	Starogroznehskaya prosp. area, hole	<1978	1430	EMP-58a	100			8				5
57	43°16, 45°45′	TCF	Oktyabr'skaya prosp. area, hole	<1978	1930	EMP-63b-1	410			12				5
57	43°16, 45°45′	TCF	Oktyabr'skaya prosp. area, hole	<1978	4500	EMP-63b-2	20			14				5
58	43°18, 46°12′	TCF	Isti-Su Spr., spring	1988	0	DB-8810	85		4410	5.7	5.7	6.6	344	7
59	43°05, 46°50′	TCF	Zuramakent (Miatly) Spr., spring	1988	0	DB-8817a	60.7	12.1	13050	10.9	3.5	5.53	300	7
59	43°05, 46°50′	TCF	Zuramakent (Miatly) Spr., spring	1988	0	DB-8817b	60			3			294	7
60	42°53, 47°15′	TCF	Zauzenbash prosp. area, hole	1988		DB-8807a	1460		130	22	22	21	311	7
61	42°43, 47°22′	TCF	El'dama settl., hole 2	1988		DB-8811	460		320	34.6	34.6	2120	297	7
62	42°52, 47°28′	TCF	Talgi Spr., hole 1-bis	1988	218–310	DB-8801a	567		5500	16.2	16.2	67	300	7
62	42°52, 47°28′	TCF	Talgi Spr., hole 1-bis	1988	218–310	DB-8801b	655	10.9	8120	17.4	17.4	66	299	7
63	42°59, 47°30′	TCF	Makhachkala thermal area, hole 220	1971	3518	ESM-27	20		30	4.6	4.5		493	1
64	42°49, 47°36′	TCF	Uytash Spr., spring	1988	0	DB-8802	1046		1890	3.4	3.4	245	296	7
65	42°24, 47°35′	TCF	Burdeki Spr., spring	1988	0	DB-8806a	95		382	4.2	4.2	142	298	7
65	42°24, 47°35′	TCF	Burdeki Spr., spring	1988	0	DB-8806b	25		600	6.7	6.7	93		7
66	42°50, 47°40′	TCF	Turali Lake region, spring	1990	0	VL-5001Б	1485	18.8	9575	2	1.5	86	297	7
67	42°21, 47°50′	TCF	Alkhadzhikent Spr., spring	1985	0	IMG-8	40		12130	33	7		291	2
68	42°31, 47°52′	TCF	Izberbash prosp. area, hole 46	1988	1200–1500	DB-8803a	43		314	5.2	5.2	95	299	7
68	42°31, 47°52′	TCF	Izberbash prosp. area, hole 46	1988	1200–1500	DB-8803b	46		470	4.3	4.3	89		7
69	42°23, 47°54′	TCF	Kayakent Spr., spring	1985	0	IMG-9	1200		9470	7.6	7		294	2
70	41°43, 48°01′	TCF	Rychal-su Spr., spring	1988	0	DB-8816	1001	1.3	1472	3.7	3.7	848	313	7
70	41°43, 48°01′	TCF	Rychal-su Spr., spring	1985	0	IMG-5	2270			4			355	2
71	42°14, 48°03′	TCF	Berikey prosp. area, hole 20	1976	1000–1500	EMP-78a	60		105	7.2	7.1		312	5
71	42°14, 48°03′	TCF	Berikey prosp. area, hole 20	1985	1000–1500	IMG-10	30			7				2
71	42°14, 48°03′	TCF	Berikey prosp. area, hole 20	1988	1000–1500	DB-8805				16	16	700	296	7
72	42°19, 48°04′	TCF	Adzhi Lake region, spring	1990	0	VL-9099	200	0.93	1830	4.3	4.3	237	300	7
73	41°34, 48°15′	TCF	Gil'yar Spr., spring	1976	0	EMP-95′	1160		450	5.3	5.3		319	5
73	41°34, 48°15′	TCF	Gil'yar Spr., spring	1985	0	IMG-6	1900			5.3				2

(Continued)

Table 1. Continued

No. in Fig. 2	Location N, E	Unit[b]	Name	Year of sample	Depth m	Sample index	He	Ne	Ar	$^3He/^4He$, 10^{-8}		$\frac{^4He}{^{20}Ne}$	$\frac{^{40}Ar}{^{36}Ar}$	Ref.
							mcc/L = ppm			meas.	corr.			
74	42°51, 44°29′	CMW	Nagutskaya settl., hole3-SG	1985	852	INK-8502a	2990		5380	47				7
74	42°51, 44°29′	CMW	Nagutskaya settl., hole3-SG	1985	852	INK8502b	3000	2.3	2170	45	45	1438	316	7
75	43°53, 42°44′	CMW	Kislovodsk Resort, hole 5-O	1989	75–147.5	DB-8907	221		625	75	75	209		7
75	43°53, 42°44′	CMW	Kislovodsk Resort, hole 5-O	1991	75–147.5	LNB9101	301	0.75	828	87	87	444	304	7
75	43°53, 42°44′	CMW	Kislovodsk Resort, hole 1-OP	1989	272	DB-8908	125	0.49	549	49	49	248	296	7
76	43°51, 42°47′	CMW	Olkhovskoe prosp. area, hole 115-E	1991		LNB9107	287	0.67	818	156	156	471	303	7
76	43°51, 42°47′	CMW	Olkhovskoe prosp. area, hole 115-bis	1991	400	LNB9108	177	0.57	713	163	163	343	298	7
78	44°01, 42°51′	CMW	Podkumok river, hole 2-NV	1986	566–580	INK-3	1499		692	87	87	176		5
79	44°03, 42°53′	CMW	Essentuki Resort, hole 418	1989	61–155	DB-8910	2290	1.38	1340	84	84	1827	320	7
79	44°03, 42°53′	CMW	Essentuki Resort, hole 418	1990	61–155	DB-9006	1420	1.6	1310	73	73	957	309	7
79	44°05, 42°53′	CMW	Essentuki Resort, hole 1CMW-bis	1986	1375–1468	INK-8615	85		133	108	108	160	297	7
79	44°05, 42°53′	CMW	Essentuki Resort, hole 1CMW-bis	1990	1375–1468	LNB9001	71	6.7	550	111	111	117	300	7
79	44°03, 42°53′	CMW	Essentuki Resort, hole 2-B	1990	958–998	LNB9003	2273	6.9	8380	67.7	68	362	300	7
79	44°03, 42°53′	CMW	Essentuki Resort, hole	<1978		EMP-97-1				78				5
80	44°02, 42°53′	CMW	Essentuki Resort, hole	1986		INK-8614	391		564	69	69	24.2		7
81	44°03, 42°53′	CMW	Essentuki Resort, hole 1-E	1990	320–462	DB-9007	3280	1.6	2450	89.3	89	2190	314	7
82	44°07, 42°53′	CMW	Novoblagodarnoe settl., hole 46	1990	552–686	DB-9010	225	0.4	531	77	77	556	306	7
83	44°05, 42°53′	CMW	Telmans settl., hole 1	<1978		EMP-97-2	1200			90				5
84	44°03, 42°53′	CMW	Essentuki Resort, hole 2-E	1989	334–435	DB-8909b	8920	6	4855	75.4	75	1521	306	7
85	44°08, 42°55′	CMW	Novoblagodarnoe settl., hole 49-A	1990	627–864	DB-9011	1400	1.5	1530	66.1	66	1024	314	7
86	44°05, 43°01′	CMW	Beshtau Mt., hole 66	1990	1632–1850	LNB9002	146	0.86	728	85.8	86	189	301	7
87	44°08, 43°02′	CMW	Zheleznovodsk Resort, hole 61	1990	209–250	LNB-61	1010	3.01	3530	43	43	368	301	7
88	44°09.43°02′	CMW	Razvalka Mt., hole 74-N	1990	1501	LNB9006	5232	8.5	10990	71.5	71	676	301	7
89	44°08, 43°02′	CMW	Zheleznovodsk Resort, hole 69	1989	277–293	DB-8914	235	0.96	1310	71	71	268	297	7
89	44°09, 43°02′	CMW	Zheleznovodsk Resort, hole 70	1990	660–1128	LNB9004	258	1.34	1420	88	88	211	302	7
90	44°08, 43°02′	CMW	Zheleznovodsk Resort, Semashko, hole	1990	59–101	DB-9009	335	1.51	1620	82	82	244	301	7
90	44°08, 43°03′	CMW	Zheleznovodsk Resort, Slavyanovskaya, hole	1990	73–120	DB-9008	128	0.78	944	73	73	180	301	7
90	44°08, 43°03′	CMW	Zheleznovodsk Resort, hole 59	1989	115–213	DB-8913	221	0.86	1170	74	74	281	299	7
91	44°06, 43°03′	CMW	Lermontov settl., hole 113	<1978		EMS-23				73				5
92	44°10, 43°06′	CMW	Zmeyka Mt., hole 72	1990	2458	LNB9005	213	0.93	1040	84.2	84	253	301	7
93	44°05, 43°04′	CMW	Pyatigorsk Resort, hole 16	1989	189–381	DB-8911a	35	0.71	960	61	60	46	296	7
93	44°05, 43°04′	CMW	Pyatigorsk Resort, hole 16	1989	189–381	DB-8911b	41.7		682.3	59	59	107		7
93	44°06, 43°04′	CMW	Pyatigorsk Resort, hole 19	1989	284–335	DB-8912	204	0.98	862	59.4	59	277	303	7
93	44°06, 43°03′	CMW	Mashuk Mt., hole 4	1990	205	DB-9003	100	0.87	812	59	59	127	298	7
93	44°07, 43°03′	CMW	Mashuk Mt., hole 24	1990	82–201	DB-9005	119	0.86	848	59.5	59	152	296	7
93	44°06, 43°04′	CMW	Mashuk Mt., hole 33-bis	1991	1337	LNB9115	178	0.7	687	63.7	64	280	300	7
94	44°06, 43°04′	CMW	Varvatsievskaya prosp. area, hole	1990	18–26	DB-9004	25.1	1.52	1125	62.8	62	18.2	294	7
95	43°51, 43°08′	CMW	Zolotoy Kurgan Mt., hole 10-KG	1985	1239–1440	INK-8501	513	21.5	12900	74	73	25.4	301	7
96	43°45, 43°08′	CMW	Shardakovo settl., hole	1985	50–60	INK-8303a	1370		1364	28	28	108		7
97	43°21, 40°16′	GC	Gagra-city, hole	<1978		EMS-50				8.9				1
98	43°31, 40°37′	GC	Avadkhara settl., hole	<1978	250	EMS-51				31				1
99	43°52, 41°10′	GC	Urup settl., hole A	<1978	300	EMP-102/1	690			59				5
99	43°52, 41°10′	GC	Urup settl., hole A	<1978	570	EMP-102/2	900			14				5
100	42°49, 41°16′	GC	Kindgi Spr., spring	1988	0	GIB8801	346	8.5	10550	34.7	34	44.5	294	7
101	43°43, 41°23′	GC	Psekencha settl., hole 68	<1978		EMS-33				47				1
102	42°44, 41°31′	GC	Okhurey Spr., spring	1988	0	GIB8802	158	6.7	9970	32.2	31	26	293	7
103	44°01, 41°33′	GC	Pregradnaya settl., hole	<1978	340	EMS-28	5890			67				1
104	43°18, 41°28′	GC	Dombay settl., hole 16	1989	128–350	DB-8901a	544	0.67	781	8	8		305	7

(Continued)

Table 1. Continued

No. in Fig. 2	Location N, E	Unit[b]	Name	Year of sample	Depth m	Sample index	He	Ne	Ar	$^3He/^4He$, 10^{-8}		$\frac{^4He}{^{20}Ne}$	$\frac{^{40}Ar}{^{36}Ar}$	Ref.
							mcc/L = ppm			meas.	corr.			
104	43°18, 41°28′	GC	Dombay settl., hole 16	1989	128–350	DB-8901b	633	1.4	1220	10	10	513	302	7
105	42°32, 44°07′	GC	Bagiata Spr., spring	<1978	0	EMP-GIB	10			650				5
106	42°30, 41°52′	GC	Zugdidi city, spring	1988	0	GIB8812	29	1.51	16500	43.7	28	2.13	298	7
107	43°47, 41°54′	GC	Karachayevsk settl., hole 114	<1978		EMS-34				7.5				1
108	44°03, 41°59′	GC	Ust-Dzheguta settl., spring	<1978	0	EMS-29				33				1
109	43°57, 41°54′	GC	Krasnogorskii Spr., spring	<1978	0	EMS-30				32				1
110	43°47, 42°00′	GC	Arbakol Spr., hole	<1978		EMS-35				100				1
111	43°46, 42°02′	GC	Garali Spr., spring	1989	0	DB-8906	7.7	0.55	549	50.6	49	15	296	7
112	43°46, 42°04′	GC	Mariinskii Narzan Spr., spring	<1978	0	EMS-36				41				1
113	42°40, 42°05′	GC	Lugella Spr., hole	<1978		EMS-52				50				1
114	43°40, 42°06′	GC	Indysh Spr., hole	<1978		EMS-37				71				1
114	43°40, 42°06′	GC	Indysh Spr., spring	1989	0	DB-8905	7	0.72	911	60.3	58	1.4	297	7
115	43°32, 42°07′	GC	Kart-Dzhiyurt Spr., spring	1989	0	DB-8904	4.6	0.57	617	183	184		293	7
116	43°05, 42°12′	GC	Tita settl., spring	<1978	0	EMS-47				54				1
117	43°57, 42°18′	GC	Krasnyi Vostok settl., hole 2-E	<1978		EMS-31				31				1
117	43°57, 42°18′	GC	Krasnyi Vostok settl., hole 2-E	1990		DB-9001	188	0.73	620	49.4	49	283	298	7
118	43°25, 42°20′	GC	Tarkhor-Narzan Spr., spring	<1978	0	EMS-40				55				1
119	43°24, 42°21′	GC	Bityuk-Tyube Spr., spring	<1978	0	EMS-39				280				1
119	43°24, 42°21′	GC	Bityuk-Tyube Spr., spring, 23 °C	1984	0	NKh-I-5	1.9		83	870				5
119	43°24, 42°21′	GC	Bityuk-Tyube Spr., spring, 15 °C	1984	0	NKh-I-4	88		4700	280				5
119	43°24, 42°21′	GC	Bityuk-Tyube Spr., spring, 8 ^{J177}C	1984	0	NKh-I-7	8		2480	230				5
120	41°57, 42°22′	GC	Nabeglavi Spr., hole 2							690				6
121	43°43, 42°31′	GC	Khasaut Spr., spring	1989	0	DB-8903	0.76	0.71	566	130	123	0.72	301	7
122	42°35, 43°12′	GC	Terskol settl., hole	<1978		EMS-41				260				1
123	42°35, 43°14′	GC	Badaevykh settl., hole	<1978		EMS-44				360				1
124	43°02, 42°36′	GC	Dalasvili Spr., spring	<1978	0	EMS-49				360				1
125	43°04, 42°37′	GC	Mazeri settl., spring	<1978	0	EMS-48				800				1
126	43°16, 42°38′	GC	Irik-Narzan Spr., spring	<1978	0	EMS-42				100				1
127	43°03, 42°40′	GC	Mestiya settl., spring	1988	0	GIB8817	2.2		510	224	243	1.6	296	7
127	43°03, 42°40′	GC	Mestiya settl., spring	<1978	0	EMP-VPY				120				7
128	43°14, 42°40′	GC	Dzhan-Tugan Spr., spring	1989	0	DB-8915	5	1.1	1300	443	458	6.5	298	7
77	43°41, 42°42′	GC	Dolina Narzanov Sprs., spring, 14 °C	1984	0	NKh-I-3	8		1040	220				5
77	43°41, 42°42′	GC	Dolina Narzanov Sprs., spring	1989	0	DB-8902	1.7	0.7	471	145	145	3	291	7
132	42°40, 42°46′	GC	Rechkhi Spr., spring	<1978	0	EMP-13′	40		9000	135				5
133	42°44, 42°48′	GC	Tsiplakakiya Spr., spring	<1978	0	EMP-GIB	40				90			5
131	43°24, 42°54′	GC	Tyrnyauz ore field, hole 104	<1978		EMS-45				360				1
129	42°48, 43°59′	GC	Gerkhozhan-Su Spr., spring	<1978	0	EMS-43				680				1
130	43°23, 43°01′	GC	Zydachit river, spring	<1978	0	EMS-46				110				1
134	44°03, 43°05′	GC	Krasnoarmeyskii settl., hole	1990	93–120	DB-9002	5.9	0.62	655	49.4	47		297	7
135	42°42, 43°17′	GC	Uravi Spr., spring	<1978	0	EMP-GIB	80				6.4			5
136	42°24, 43°56′	GC	Dzhava Spr., spring	<1978	0	EMP-GIB	150				330			5
136	42°24, 43°56′	GC	Dzhava Spr., spring	1988	0	GIB8816	23		7500	174	215	0.55	293	7
137	43°04, 42°41′	GC	Artskheli Spr., spring	<1978	0	EMP-GIB					82			5
138	42°50, 44°03′	GC	Sadon ore field, mine 8	<1978		EMS-38				6.7				1
139	42°34, 44°04′	GC	Truso Spr., spring	1983	0	1-375-84	20		590	260				7
140	42°23, 44°38′	GC	Nadibaani Spr., spring		0					660				6
141	42°27, 44°39′	GC	Pansheti Spr., spring	<1978	0	EMP-GIB					250			5
142	42°21, 44°41′	GC	Pasanauri Spr., hole 9							300				6

(Continued)

Table 1. Continued

No. in Fig. 2	Location N, E	Unit[b]	Name	Year of sample	Depth m	Sample index	He	Ne	Ar	$^3He/^4He$, 10^{-8}		$\frac{^4He}{^{20}Ne}$	$\frac{^{40}Ar}{^{36}Ar}$	Ref.
							mcc/L = ppm			meas.	corr.			
143	42°23, 44°47′	GC	Makarta Spr., spring	<1978	0	EMP-GIB	30				690			5
144	42°35, 45°07′	GC	Datvisi Spr., spring	1988	0	GIB8803	1140		860	193	193	1600	416	7
145	42°40, 45°09′	GC	Khakhmati Spr., spring	1988	0	GIB8804	8.5		760	355	366	5.9	293	7
146	42°45, 45°36′	GC	Itum-Kale, spring	1989	0	MKK-89	0.67	0.92	681	145	148	0.8	299	7
147	42°26, 45°59′	GC	Za-Echeda Spr., spring	1988	0	DB-8809a	56		4340	159	159	42	303	7
147	42°26, 45°59′	GC	Za-Echeda Spr., spring	1988	0	DB-8809b	20		6620	155	230	0.36		7
148	42°24, 46°02′	GC	Inkhokvari Spr., spring	1985	0	IMG-1	10			35				2
149	42°07, 46°06′	GC	Khzan-Or Spr., spring	<1978	0	EMP-32	7380		4560	5.3	5.3		345	7
149	42°07, 46°06′	GC	Khzan-Or Spr., spring	1985	0	IMG-2	10670			5.3			415	2
150	41°22, 47°28′	GC	Khnov settl., “New” spring	1988	0	DB-8813	1820		4660	3.1	3.1	556	296	7
150	41°22, 47°28′	GC	Kizil-dere ore field, hole	21.7.76		134	930			3.8				4
150	41°22, 47°28′	GC	Kizil-dere ore field, hole	25.7.76		138	920			4				4
150	41°22, 47°28′	GC	Kizil-dere ore field, hole	28.7.76		141	800			4				4
150	41°22, 47°28′	GC	Kizil-dere ore field, hole	29.7.76		142	820			3.8				4
150	41°22, 47°28′	GC	Kizil-dere ore field, hole	31.7.76		144	850			3.6				4
150	41°22, 47°28′	GC	Kizil-dere ore field, hole	10.8.76		154	720			4.4				4
150	41°22, 47°28′	GC	Kizil-dere ore field, hole	16.8.76		160	800			3.6				4
150	41°22, 47°28′	GC	Kizil-dere ore field, hole	23.8.76		167	870			4.3				4
150	41°22, 47°28′	GC	Kizil-dere ore field, hole	1.9.76		176	860			3.5				4
150	41°22, 47°28′	GC	Kizil-dere ore field, hole	3.9.76		178	870			3.9				4
150	41°22, 47°28′	GC	Kizil-dere ore field, hole	10.9.76		184	860			4.2				4
150	41°22, 47°28′	GC	Kizil-dere ore field, hole	<1978		EMP-33	850		1380	2.5	2.4		327	7
150	41°22, 47°28′	GC	Kizil-dere ore field, hole 221	1985		IMG-3	860			5.5			606	2
150	41°22, 47°28′	GC	Kizil-dere ore field, hole 315	1988		DB-8812a	12650		4690	4.2	4.2	310	296	7
150	41°22, 47°28′	GC	Kizil-dere ore field, hole 315	1988		DB-8812b	4840	3.2	1990	3.5	3.5	1665	336	7
151	41°28, 47°43′	GC	Dzhani settl., spring	1985	0	IMG-4	6880		2380	14	14		322	2
151	41°28, 47°43′	GC	Dzhani settl., hole	1988		DB-8815	7366	3.6	2230	2.3	2.3	2268	315	7
152	41°28, 47°46′	GC	Khkem settl., Gazovaya balka, hole	1988		DB-8814a	1650		534	2.4	2.4	3390	295	7
152	41°28, 47°46′	GC	Khkem settl., Gazovaya balka, hole	1988		DB-8814b	1900	1.13	1100	2.9	2.9	1841	314	7

[a] All available data (including lab duplicates) are presented without any averaging.
[b] Tectonic Units: SP—Scythian plate, Sa—Stavropol arch, IKF—Indol-Kuban foredeep, TCF—Terek-Caspian foredeep, CMW—Caucasian Mineral Waters area, GC—Greater Caucasus.
1—[Matveeva et al., 1978]; 2—[Gasaliev and Prasolov, 1988]; 3—[Lavrushin et al., 1966]; 4—[Prasolov, 1990]; 5—[Polyak et al., 1997]; 6—[Buachidze and Mkheidze, 1989]; 7—this work.

Table 2. Major gases abundances in the Northern Caucasus subsurface fluids.

## Fig. 2	Unit[a]	Sampling site	Year of sampling	Sampling point	Depth m	H2	O2	N2	CO2	CH4	Ref.[b]
						in 10^4 mcc/L = 10^4 ppm					
29	IKF	Begol Spr.	1968	Spring	0			1.7	47.8	50.5	1, 2
30	IKF	Priozernaya prosp. area	1968	Hole			0.30	3.3	5.0	88.9	1, 2
31	IKF	Andrusova mud v.	1968	Spring	0			0.8	8.6	90.6	1, 2
31	IKF	Oldenburgskogo mud v.	1968	Spring	0			0.6	8.0	91.4	1, 2
31	IKF	Trubetskogo mud v.	1968	Spring	0			0.3	59.5	40.2	1, 2
32	IKF	Karabetova gora mud v.	1990	Spring	0	0.0009	0.034	0.91	20.9	77.5	3
32	IKF	Karabetova gora mud v.	1968	Spring	0			0.6	0.3	99.1	1, 2
33	IKF	Kuchugurskii mud v.	1994	Spring	0	tr.	0.095	0.74	29.2	69.9	3
34	IKF	Yuzhno-Bugazskii mud v.	1968	Spring	0			0.9	2.0	97.1	1, 2
35	IKF	Shapurskii mud v.	1994	Spring	0	0.0009	0.061	0.81	6.7	92.0	3
36	IKF	Polivadina mud v.	1994	Spring	0	0.0009	0.099	0.73	13.1	85.8	3
37	IKF	Zapadnyi Tsimbaly mud v.	1994	Spring	0	<0.00006	0.065	1.32	<0.004	97.2	3
38	IKF	Vostochnyi Tsimbaly mud v.	1994	Spring	0	0.0009	0.017	0.94	<0.004	95.8	3
39	IKF	Akhtanizovskii mud v.	1994	Spring	0	<0.00006	0.065	1.91	14.4	82.5	3
40	IKF	Sinyaya Balka mud v.	1994	Spring	0	<0.00006	0.082	1.31	tr.	94.1	3
42	IKF	Sopka mud v.	1994	Spring	0	<0.00006	0.08	2.06	6.4	91.1	3
43	IKF	Severo-Neftyanoi mud v.	1994	Spring	0	<0.00006	0.027	1.17	5.6	90.1	3
44	IKF	Yuzhno-Neftyanoi mud v.	1994	Centr. spring	0	0.0066	0.068	0.88	6.3	82.3	3
44	IKF	Yuzhno-Neftyanoi mud v.	1994	East. spring	0	0.0006	0.078	1.51	15.8	82.1	3
45	IKF	Golubitskii morskoy m.v.	1994	Spring	0	0.009	0.19	1.67	<0.004	91.8	3
46	IKF	Miska mud v.	1994	Spring	0	<0.00006	0.150	3.85	<0.004	91.1	3
47	IKF	Semigorskii mud v.	1994	Spring	0	tr.	0.082	1.62	3.4	94.8	3
48	IKF	Shugo mud v.	1994	Spring 1	0	<0.00006	0.095	0.92	8.5	89.5	3
49	IKF	Gnilaya Sopka mud v.	1994	East. spring	0	<0.00006	0.088	1.47	<0.004	92.6	3
50	IKF	Gladkovskii mud v.	1994	Spring	0	tr.	0.16	4.64	<0.004	94.2	3
51	IKF	Kievskii mud v.	1994	Spring	0	0.0012	0.08	0.88	7.3	91.4	3
59	TCF	Zuramakent (Miatly) Spr.	<1988	Spring	0	0.005	0.2	90.5	6.0	3.2	5
60	TCF	Zauzenbash prosp. area	1988	Hole			0.2	1	5.9	92.8	6
61	TCF	El'dama settl.	1988	Hole 2			0.35	8.5	4.7	86.3	6
64	TCF	Uytash Spr.	1988	Spring	0		0.03	42.2	9.9	47.3	6
65	TCF	Burdeki Spr.	1988	Spring	0			3.2	3.0	93.8	6
67	TCF	Alkhadzhikent Spr.	<1988	Spring	0	0.001	0.4	97.3	1.8	1.3	5
68	TCF	Izberbash prosp. area	<1984	Hole 46	1200–1500		0.8	18.1	3.7	77.2	4
69	TCF	Kayakent Spr.	<1988	Spring	0		0.75	92.9	5.8	0.3	5
70	TCF	Rychal-su Spr.	<1988	Spring	0		0.1	13.2	22.6	63.9	5
71	TCF	Berikey prosp. area	<1988	Hole 20	1000–1500	0.004	0.5	2.4	93.0	3.9	5
73	TCF	Gil'yar Spr.	<1988	Spring	0		1.6	11.7	5.0	81.5	5
75	CMW	Kislovodsk Resort	1989	Hole 5-O	75–147.5		0.8	3.9	95.2	0.01	6
75	CMW	Kislovodsk Resort	<1972	Hole 5-O	75–147.5		0.02	1.73	98.2	0.03	7
75	CMW	Kislovodsk Resort	<1971	Hole 1-OP	272		0.28	6.07	93.7		8
77	GC	Dolina Narzanov (Narzan valley)	<1972	Spring	0			0.92	99.1		7
77	GC	Dolina Narzanov (Narzan valley)	1989	Spring	0		0.6	2.2	97.2		6
79	CMW	Essentuki Resort	1989	Hole 418	61–155			1.6	69.6	28.1	6
79	CMW	Essentuki Resort	1989	Hole 2-E	334–435		0.1	18.7	59.8	21.0	6
79	CMW	Essentuki Resort	1990	Hole 1-E	320–462			22.3	51.7	25.0	6
79	CMW	Essentuki Resort	1990	Hole 1KMWbis	1375–1468			0.9	99.0	0.04	6
79	CMW	Essentuki Resort	1990	Hole 2-B	958–998			34.9	63.8	0.33	6
82	CMW	Novoblagodarnoe settl.	1990	Hole 46	552–686			14.6	65.3	20.0	6

(Continued)

Table 2. Continued

## Fig. 2	Unit[a]	Sampling site	Year of sampling	Sampling point	Depth m	H2	O2	N2	CO2	CH4	Ref.[b]
						in 10^4 mcc/L = 10^4 ppm					
85	CMW	Novoblagodarnoe settl.	1990	Hole 49-A	627–864			10.3	46.8	42.3	6
86	CMW	Beshtau Mt.	<1990	Hole 66	1632–1850			1.4	98.1	0.33	6
88	CMW	Razvalka Mt.	<1990	Hole 74-N	1501			47	51.0	2.0	9
90	CMW	Zheleznovodsk Resort, Semashko	1990	Hole	59–101			4.7	95.0	0.047	6
90	CMW	Zheleznovodsk Resort, Slavyanovskaya	1990	Hole	73–120			3.6	96.6	0.3	6
90	CMW	Zheleznovodsk Resort	1989	Hole 59	115–213		1.4	4.8	93.2	0.48	6
90	CMW	Zheleznovodsk Resort	1990	Hole 61	209–250			20.7	1.4	77.4	6
90	CMW	Zheleznovodsk Resort	1989	Hole 69	277–293		0.7	10.2	88.8	0.13	6
90	CMW	Zheleznovodsk Resort	1990	Hole 70	660–1128			0.21	97.7	2.03	6
92	CMW	Zmeyka Mt.	<1990	Hole 72	2458			2.0	98.0		9
93	CMW	Pyatigorsk Resort	1989	Hole 16	189–381		0.1	4.0	95.6	0.09	6
93	CMW	Pyatigorsk Resort	1989	Hole 19	284–335	<0.001	4.7	18.2	75.4	1.22	6
93	CMW	Mashuk Mt.	1990	Hole 4	205	0.0026	4.3	26.2	68.4	0.04	6
93	CMW	Mashuk Mt.	1990	Hole 24	82–201	<0.001	3.6	14.2	82.0	0.14	6
93	CMW	Mashuk Mt.	<1972	Hole 33bis	1337		0.07	1.1	98.5	0.08	7
94	CMW	Varvatsievskaya prosp. area	1990	Hole	18–26			4.6	95.2	0.036	6
97	GC	Gagra-city[c]	<1975	Hole				74.7	24.7	0.6	10
98	GC	Avadkhara settl.	<1975	Hole 6	700			3.3	96.7		10
106	GC	Zugdidi city	<1975	Hole 4				55.6	43.5	0.9	10
114	GC	Indysh Spr.	1989	Spring	0		0.5	1.5	98.0		6
115	GC	Kart-Dzhiyurt Spr.	1989	Spring	0		6.5	10.9	77.1		6
121	GC	Khasaut Spr.	1989	Spring	0		0.4	0.8	98.8		6
134	GC	Krasnoarmeyskii settl.	1990	Hole	93–120		1.9	6.6	91.5	0.01	6
136	GC	Dzhava Spr.	<1975	Hole 44	120–280			63.4	29.7	6.9	10
136	GC	Dzhava Spr.	<1975	Hole 14A					97.7		10
139	GC	Truso Spr.	<1975	Spr. Styr-suar	0			1.5	97.9	0.6	10
141	GC	Pansheti Spr.	<1975	Spring	0			9.2	90.8		10
145	GC	Khakhmati Spr.	<1975	Spring	0			2.2	97.8		10
148	GC	Inkhokvari Spr.	<1988	Spring	0	0.002	0.4	11.5	87.9	0.2	5
149	GC	Khzan-Or Spr.	<1988	Spring	0		0.3	61.5	2.9	34.2	5
150	GC	Kizil-dere ore field	<1988	Hole 221			0.2	9.9	1.4	88.4	5
151	GC	Dzhani settl.	<1988	Spring	0		0.4	25.3	4.0	70.1	5

[a] Tectonic Units: IKF—Indol-Kuban foredeep, TCF—Terek-Caspian foredeep, CMW—Caucasian Mineral Waters area, GC—Greater Caucasus.

[b] 1—[Gemp et al., 1979]; 2—[Lagunova, 1974]; 3—[Lavrushin et al., 1996]; 4—[Voitov et al., 1984]; 5—[Gazaliev and Prasolov, 1988]; 6—this work; 7—[Ivanov, 1972]; 8—[Shcherbak and Gurevich, 1971]; 9—[Trebukhova and Chesalov, 1990]; 10—[Buachidze, 1975].

[c] Water-dissolved gas.

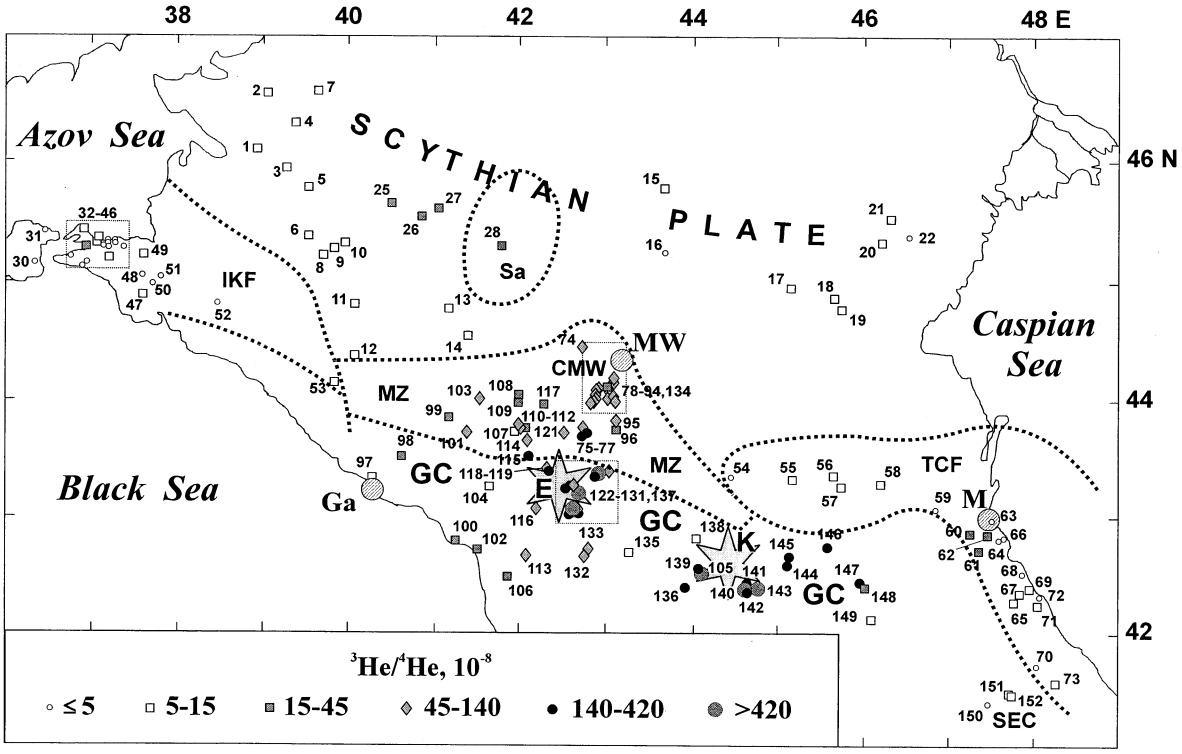

Fig. 2. Location map of the sampling sites in the Northern Caucasus (site numbers correspond to those in Tables 1 and 2). Tectonic units: (GC) Greater Caucasus meganticlinorium, (SEC) its south-eastern sector, (MZ) monocline zone, (Sa) Stavropol arch, (IKF) Indol-Kuban foredeep, (TCF) Terek-Caspian foredeep, (CMW) Caucasian Mineral Waters area. Stars mark the Elbrus (E) and Kazbek (K) volcanic centres; dashed circles denote the cities Mineral'nye Wody (MW), Makhachkala (M), and Gagra (Ga).

shadowed arrow. Mechanisms causing a substantial horizontal scatter of CMW data-points were already discussed above.

In the Kazbek vicinity, CO_2 is even isotopically heavier than that of the CMW fluids: the mean $\delta^{13}C$ value in CO_2 equals to −1.9‰ (Buachidze and Mkheidze, 1989). This indicates a higher contribution of crustal CO_2 in fluids due to metamorphic processes initiated by igneous activity.

The Indol-Kuban (IKF) and Terek-Caspian (TCF) foredeeps contain methane-bearing gases. *R*-values are of crustal (radiogenic) level, excepting three sites from the TCF: Zauzenbash ($R = 22 \times 10^{-8}$), Eldama (35×10^{-8}), and Talgi (16×10^{-8}). The crustal *R*-values are also typical of a few N_2- and CO_2-bearing manifestations: the Berikey borehole and Zuramakent, Kayakent, and Alkhadzhikent thermal springs in TCF, and Trubetskogo mud volcano in IKF. Gases from the oil/gas-bearing Scythian plate show *R*-values slightly above the canonical radiogenic value, 2×10^{-8}.

Both foredeeps and Scythian plate do not show statistically significant *R*–[He] correlations (Fig. 3). A great [He] range observed in these areas reflects different production of methane and radiogenic helium in sedimentary rocks as well as their loss from this reservoir.

CO_2 and CH_4-bearing gases usually contain N_2, but nitrogen is the major component in a few samples only. Data-points in N_2 versus Ar_{air} plot generally follow the solubility trend originated from dilution of the atmospheric species by carbon dioxyde or methane (Fig. 4). Some points shift from this trend indicating both underground generation of nitrogen or consumption of presumably atmospheric N_2. Thus, helium isotopic compositions shed little light on processes governed behaviour of nitrogen.

5.2. He Isotopes, Tectonics and Magmatism

5.2.1. Cis-Caucasian foredeeps and Scythian plate

Regularities of lateral *R* variations are best seen from the bar charts for specified tectonic units (Fig. 5). The lowest average R_{av}-values characterise Indol-Kuban (5.2×10^{-8}) and Terek-Caspian (5.6×10^{-8}) foredeeps filled by Alpine molasse. Three Daghestan sites in the Terek-Caspian (Zauzenbash, Eldama and Talgi) show enhanced *R*. These sites are associated with apparent trust fault (see C-D cross section in Fig. 1) and a local zone of recent extension (Koronovsky, 1994), so mantle derivatives could migrate upward. When the relevant *R*-values are excluded from the Terek-Caspian data, both foredeeps show statistically indistinguishable R_{av}-values, with a general R_{av}[1] = $(5.36 \pm 0.73) \times 10^{-8}$. Similar values are observed in the Trans-Caucasian depressions ($R_{av} = 5.58 \times 10^{-8}$) and in the West European segment of the Alpine belt, e.g., in the Cis-Alpine Molasse foredeep, $R_{av} = (5.84 \pm 1.36) \times 10^{-8}$, the Dosso Degli Angelli gas field, and the Po basin, $R_{av} = (4.96 \pm$

[1] Here and below the error was estimated as $\pm 1.96 \times S/N^{0.5}$ where S and N denote standard deviation and number of particular values, respectively.

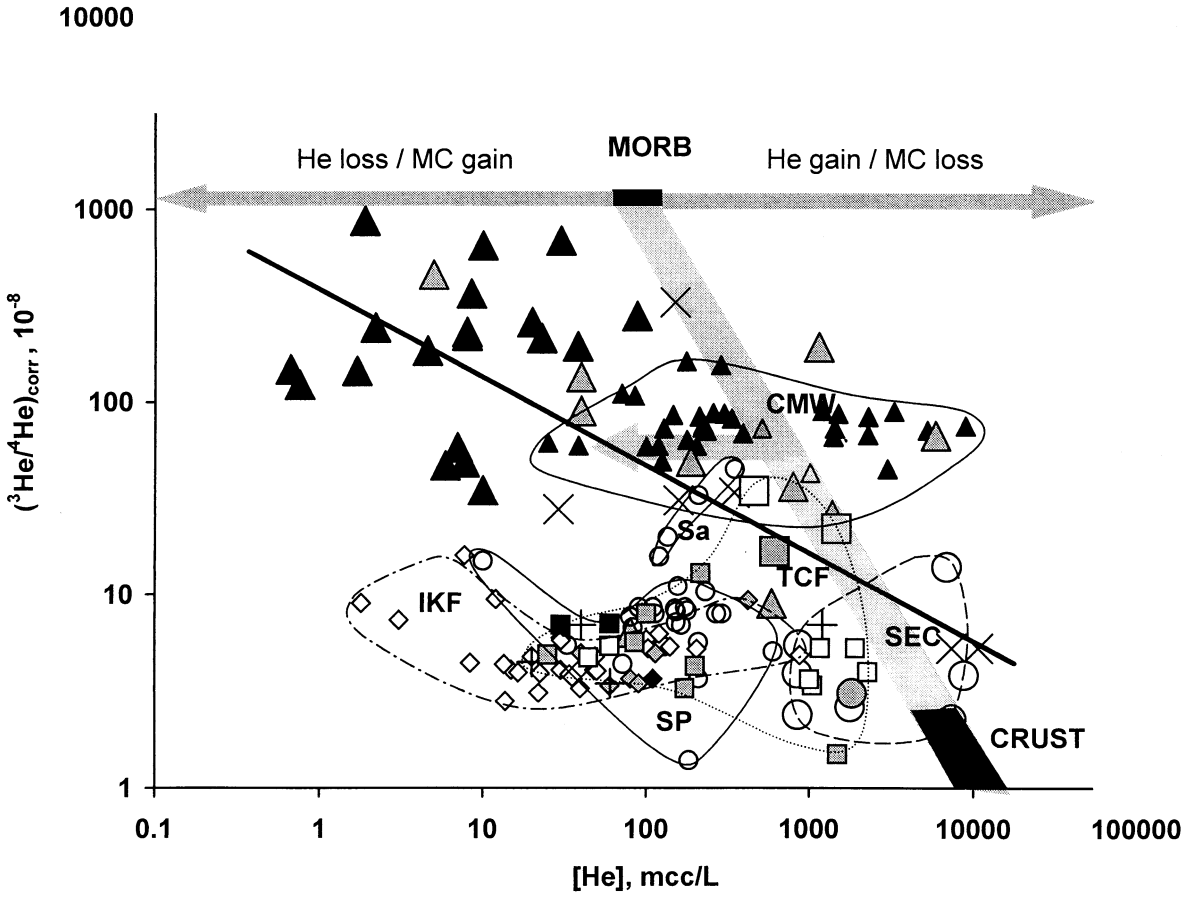

LEGEND

Tectonic unit	Abbreviation	Predominant component in gas phase			
		CO_2	CH_4	N_2	unknown
Greater Caucasus and monocline zone	GC+MZ	▲		×	△
Caucasian Mineral Waters area	CMW	▲	△		△
South-eastern part of Greater Caucasus	SEC		○		●
Indol-Kuban Foredeep	IKF	◆	◇		
Terek-Caspian Foredeep	TCF	■	□	+	▨
Daghestan anomalies			□		▨
Scythian Plate	SP		○		
Stavropol arch	Sa		○		

Fig. 3. Relationships between helium isotope compositions and concentrations in fluid gas phase (see legend for symbols). The black rectangle shows a hypothetical MORB-like end-member (Marty and Tolstikhin, 1998). Dark rhomb corresponds to a crustal helium reservoir. Slope band between these rectangles reflects mixing between the crustal (almost ^{3}He-free) helium and the fluid with MORB-like $CO_2/^3$He ratio. Horizontal shadowed trends are explained it the text. Statistical analyses of the data has shown that there is no *R*-[He] correlation in mainly CH_4-rich fluids from oil/gas-bearing provinces, both foredeeps and Scythian Plate (beyond the Stavropol arch). CO_2-rich gases from the CMW area also do not show the correlation. Four measurements from the Stavropol arch and its north-western vicinity show direct correlation, probably reflecting mixing of fluids from SP and CMW. In contrast, mainly CO_2-bearing gases from the Greater Caucasus show the statistically significant inverse *R*-[He] correlation (solid regression line).

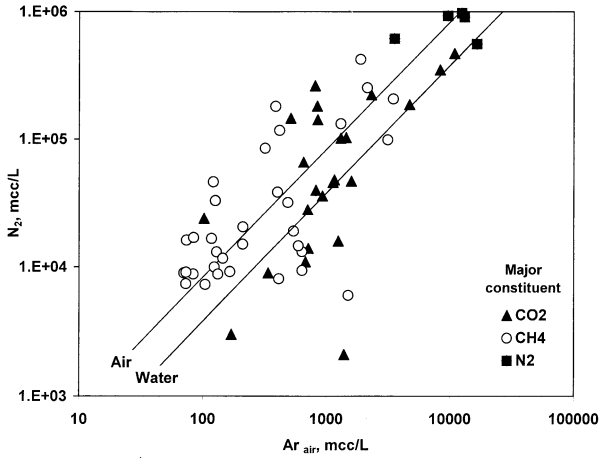

Fig. 4. Relationships between nitrogen and atmospheric argon concentrations. Data points mainly follow the solubility trend, but there are some substantial deviations also, showing both consumption of presumably air nitrogen and undergoing nitrogen generation.

0.30) $\times$ 10^{-8} (Polyak et al., 1979a; Oxburgh et al., 1986; Marty et al., 1992; Elliot et al., 1993).

Gases from the Scythian plate beyond the Stavropol arch (Fig. 5) contain He with R_{av} = (7.51 $\pm$ 1.08) $\times$ 10^{-8} which is indistinguishable from that observed in the Paris Basin, R_{av} = (8.79 $\pm$ 1.06) $\times$ 10^{-8}, which has a basement of the same Hercynian age (Marty et al., 1993). These ratios are slightly higher than the canonical radiogenic production ratio of $\approx$2 $\times$ 10^{-8} typical for Precambrian platforms (Mamyrin and Tolstikhin, 1984). Polyak and Tolstikhin (1985) considered this difference as a result of ageing of crustal domains. Marty et al. (1993) proposed a contribution of mantle-derived helium in Paris Basin fluids from either migration of volatiles from the Massif Central (Matthews et al., 1987) or extensional tectonism during upper Palaeozoic time. However, recent careful studies of He isotope and relevant trace element inventories in rocks and mineral separates have shown that enhanced (relative to the canonical production) *R*-values, up to $\sim$10$\times$$10^{-8}$, could originate from specific composition of sediments, e.g., high Li concentrations in shales or a long residence time of ^{3}H (and ^{3}He) in some chemical sediments (Loosli et al., 1995; Tolstikhin et al., 1996; Tolstikhin et al., 1999). Therefore, to adequately interpret enhanced *R*-values, the He-productive potential of host rocks (both aquifers and aquitards) in a given region must be examined.

5.2.2. *Stavropol arch—CMW area:* R *anomaly*

R-values are increasing from the northern periphery of the Stavropol arch, 1.6 $\times$ 10^{-7}, towards its central part, 4.5 $\times$ 10^{-7}. These values indicate a small contribution of mantle-derived helium. However, volcanic manifestations are not known here.

The CMW area, situated to the south of Stavropol arch, has been studied in detail: 37 specimens from 34 objects have been analysed (Tables 1, 2). *R* varies within relatively narrow limits with R_{av} = (7.64 $\pm$ 0.88) $\times$ 10^{-7} (Fig. 5). Within this area there are several $\approx$8 Ma old laccolites. Several local *R*-fluctuations correlate with neither distances from laccolithes nor

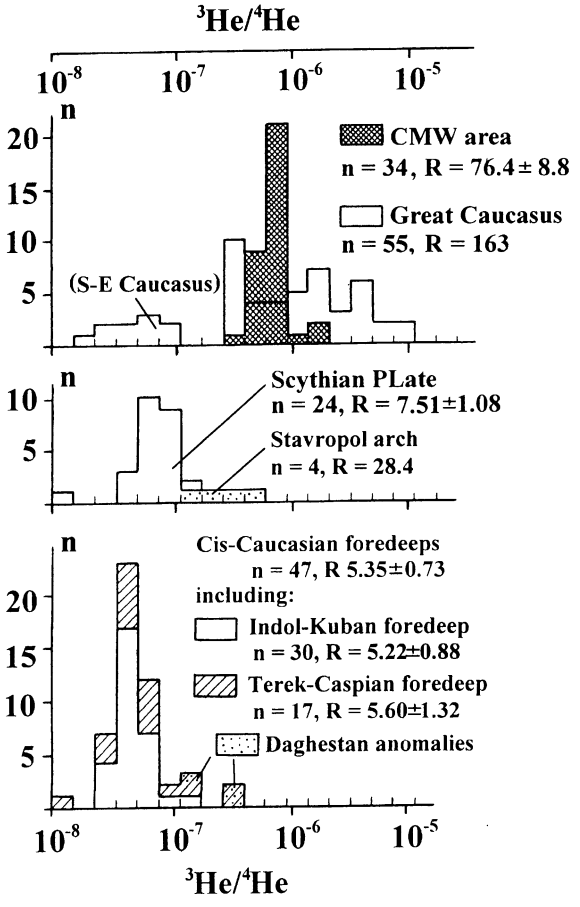

Fig. 5. Bar charts of the *R* distribution in different tectonic units of the Northern Caucasus.

lithological-stratigraphycal characteristics of aquifers. Southward of the CMW area *R* further increases up to 0.87 $\times$ 10^{-5} in Bityuk-Tyube Springs nearest to the Elbrus volcano.

Yakovlev and Polyak (1998) studied mechanism responsible for this near-longitudinal trend. Based on hydrological modelling, these authors concluded that the trend extending so far from the active volcano can not be attributed to a lateral migration of magmatic fluids from a single volcanic feeder.The enhances ^{3}He/^{4}He halo encompassed not only the central segment of the Greater Caucasus but the adjacent part of the Scythian Plate as well, mainly results from degassing of deep-seated magmatic reservoirs situated far to the north of Elbrus.

5.2.3. R *distribution along the Greater Caucasus*

In the fluids of the Greater Caucasus as a whole, the *R* spectrum is very wide (see Fig. 5). The highest *R* are concentrated around the Elbrus and Kazbek volcanoes separated by relatively low *R*-values measured in the Sadon and Uravi sites (Table 1, Fig. 6a). These sites are situated on the northern and southern slopes of the range, respectively, in a transversal compression zone predicted by tectono-physical modelling (Koronovsky, 1994). The enhanced *R*-values occur not only nearby N-Q volcanic manifestations, but also far away along

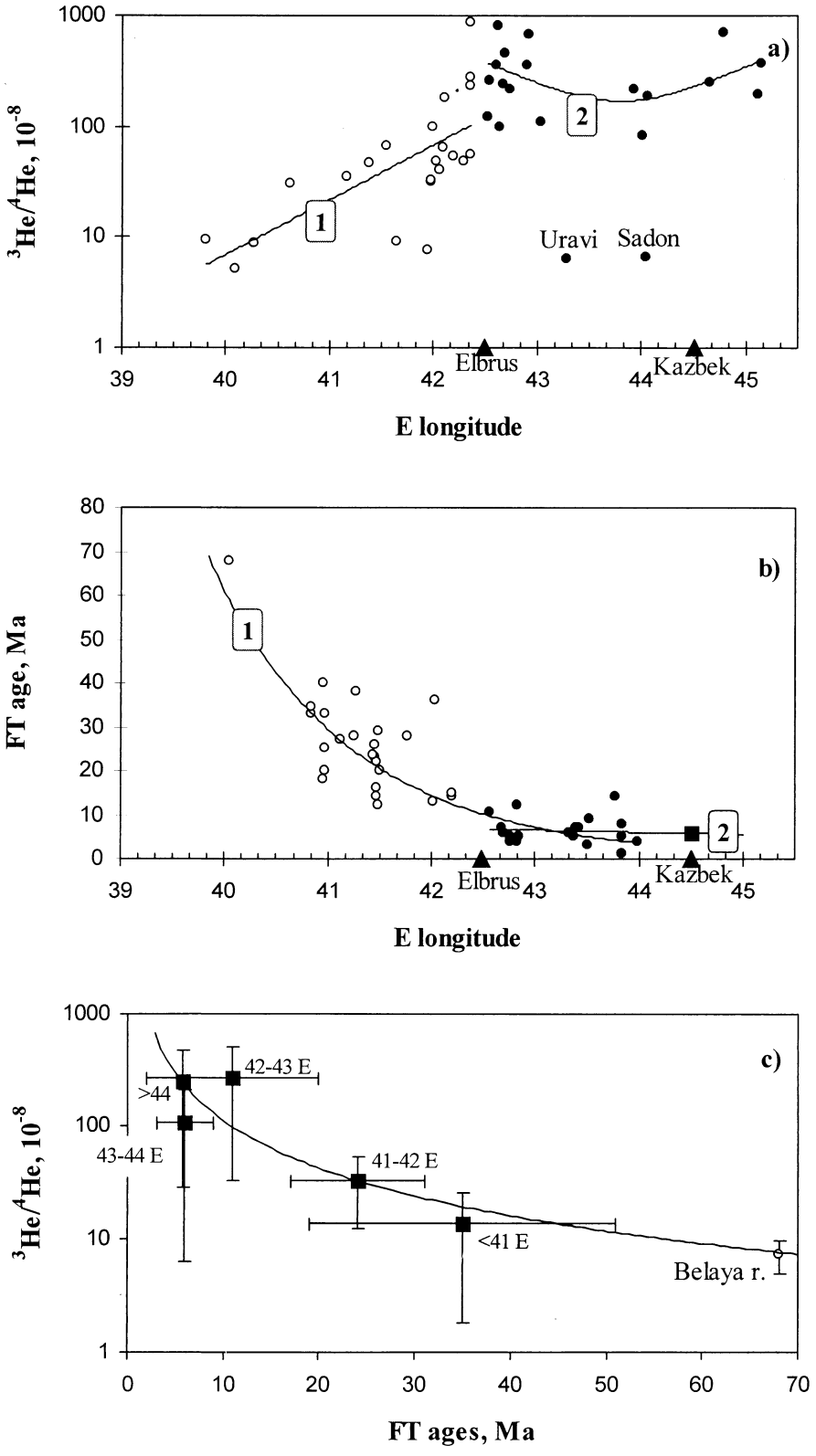

Fig. 6. Relationship between the apatite fission track ages for pre-Alpine basement of the Greater Caucasus orogene, FT-ages (Kral and Gurbanov, 1996) and the helium isotope composition in spring gases. Longitudinal trends of (a) R and (b) FT ages; (c) correlation between the averaged R and FT-ages in 1°-longitudinal sectors of the Greater Caucasus ($r_{R/FT} = 0.887 > 0.878 = r_{0.05,\, f = k-2}$), squares mark the means, open circle corresponds to the single FT-age value for Belaya River area; errors are 1σ.

the orogene where recent magmatism is not observed on the surface.

To the west of the Elbrus, decreasing *R*-values correspond to increasing fission track ages (Fig. 6b) available for the pre-Alpine basement of the orogene (Kral and Gurbanov, 1996). An inverse correlation between these parameters is quite clear after their averaging in the longitudinal segments of the orogene (Fig. 6c).

Kral and Gurbanov (1996) believed that fission track ages correspond to the time of uplifting of basement blocks through the isotherm which allows fission tracks in apatite to be retained; therefore they suggested a sequential uplifting of longitudinal segments from the west to the east. Judging from helium isotope data, such an uplifting could be provoked by upward movements of mantle matter.

However, an alternative interpretation is also possible: gradual cooling of the Greater Caucasus, treated as a single body, from the eastern and western segments towards to the central one. Such a cooling could reflect reduction of island-arc magmatic activity in the marginal segments, whereas it is still preserved in the centre, beneath Elbrus-Kazbek zone. Subsequent uplifting and erosion exposed both earlier-cooled marginal blocks and the later-cooled ones situated closer to centre: the close to the centre, the later the cooling, the younger fission track ages, and the higher *R*-values. This interpretation is in accord with the general *R*-age relationship (Polyak et al., 1979a; Polyak and Tolstikhin, 1985; Polyak, 1988).

Unlike the Alps (Marty et al., 1992), in the Caucasus there is no relation between the isotopic composition of fluid helium and crustal thickness. Moreover, some of the highest *R*-values are observed in the areas with the maximum depth(s) to the Moho discontinuity. So, the crustal thickness does not control the contribution of mantle-derived species introduced into the crust, but intrusion of mantle melts appears to be important.

5.2.4. He-Sr isotopic systematics

The Elbrus calc-alcaline acidic rocks were considered as products of anatexis in a granite-metamorphic layer (e.g., Milanovsky and Koronovsky, 1973). However, the Sr-Nd-O isotope systematics implies a mantle source for recent volcanic rocks and their substantial contamination with crustal material (Ivanov et al., 1993; Bubnov et al., 1995). The contamination of the Elbrus lavas with $^{87}Sr/^{86}Sr$ ratio ranging from 0.70528 to 0.70590 (ibid.) appears to be lower than the CMW trachyrhyolites, where this ratio varies from 0.70754 to 0.70851[2] (Pohl et al., 1993).

Figure 7 shows an inverse correlation between $^{87}Sr/^{86}Sr$ ratios in the rocks and *R* in fluids from the Elbrus and CMW areas, similar to that observed for Italian volcanic rocks and fluids (Polyak et al., 1979b). Such a correlation implies a transfer of He and Sr from the mantle by melts; and contamination of mantle melts by crustal components with contamination being greater within the CMW area than beneath the Elbrus.

[2] Values of initial ratio after correction for ^{87}Rb decay during 8.25 Ma [ibid.]

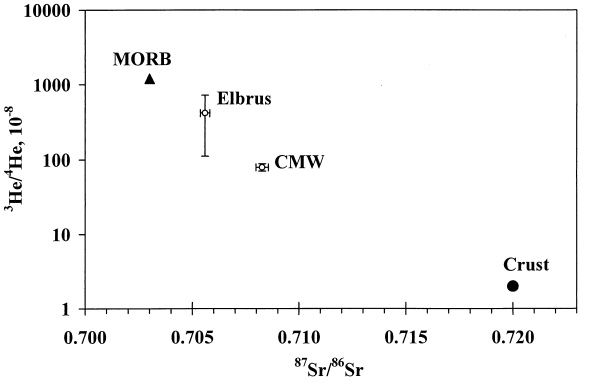

Fig. 7. Relationship between $^3He/^4He$ in fluids and $^{87}Sr/^{86}Sr$ in volcanic rocks from the Elbrus and CMW areas. Errors are 1 σ. The data for MORB and crustal reservoirs (Mamyrin and Tolstikhin, 1984; Faure and Powell, 1972) are shown for comparison.

5.3. Correlation between the *R* and Heat Flow

The terrestrial heat flow expresses an integral energetic effect of all processes occurring at depths. The flow density, *q*, measured in an individual borehole is usually disturbed by many factors (local topography, climatic changes, groundwater circulation, variability of thermal properties of rocks, sedimentation, thrusting, etc.). In order to estimate an undisturbed *q*-value, the contributions of above-mentioned factors must be quantified which is hard to do reliably in most cases. Regional averaging within a given tectonic unit allows influence of some of these factors to be eliminated. The averaged values q_{av} do indicate some regular correlation between q_{av} and the age of magmatic activity (thermal events) in lithosphere (Polyak and Smirnov, 1968; Sclater and Francheteau, 1970; Chapman and Pollack, 1976; Sclater et al., 1981, and others).

Several maps of the heat flow density within the Caucasus were compiled (Hurtig, 1992; Kutas, 1993; Moisseenko and Negrov, 1993). Figure 8 reproduces fragments of these maps. The Cis-Caucasian foredeeps show a reduced heat flow density (Fig. 8a), $q_{av} = 52 \pm 0.8$ mW/m^2 (Smirnov et al., 1992), with local positive anomalies; one of these coincides with the Daghestan enhanced *R*-values noted above.

The Scythian plate differs from the foredeeps by an elevated $q_{av} = 62 \pm 0.6$ mW/m^2 (Smirnov et al., 1992) with even higher $q_{av} = 93 \pm 1.7$ mW/m^2 for the Stavropol arch. Polyak and Smirnov (1968) considered the Stavropol anomaly to be a result of recent magmatism. A substantial contribution of mantle-derived helium to arch fluids does support this interpretation.

In the Greater Caucasus meganticlinorium both *R* and *q* are enhanced, although the heat flow distribution is rather complicated here. Low $q < 40$ mW/m^2 is typical of the south-eastern segment (Fig. 8a) and correspond to the low crustal *R*-values, $(2.3–5.3) \times 10^{-8}$, in methane- and nitrogen-bearing fluids. These fluids most likely originate from degassing of recent molasse sediments overthrusted by Mesozoic to Paleogene sedimentary rocks of the Caucasus orogene (see Fig. 1c). Simultaneously, the thrusting should decrease *q* in upper horizons. There is no generally accepted pattern of heat flow density distribution in the central segment, as follows from a

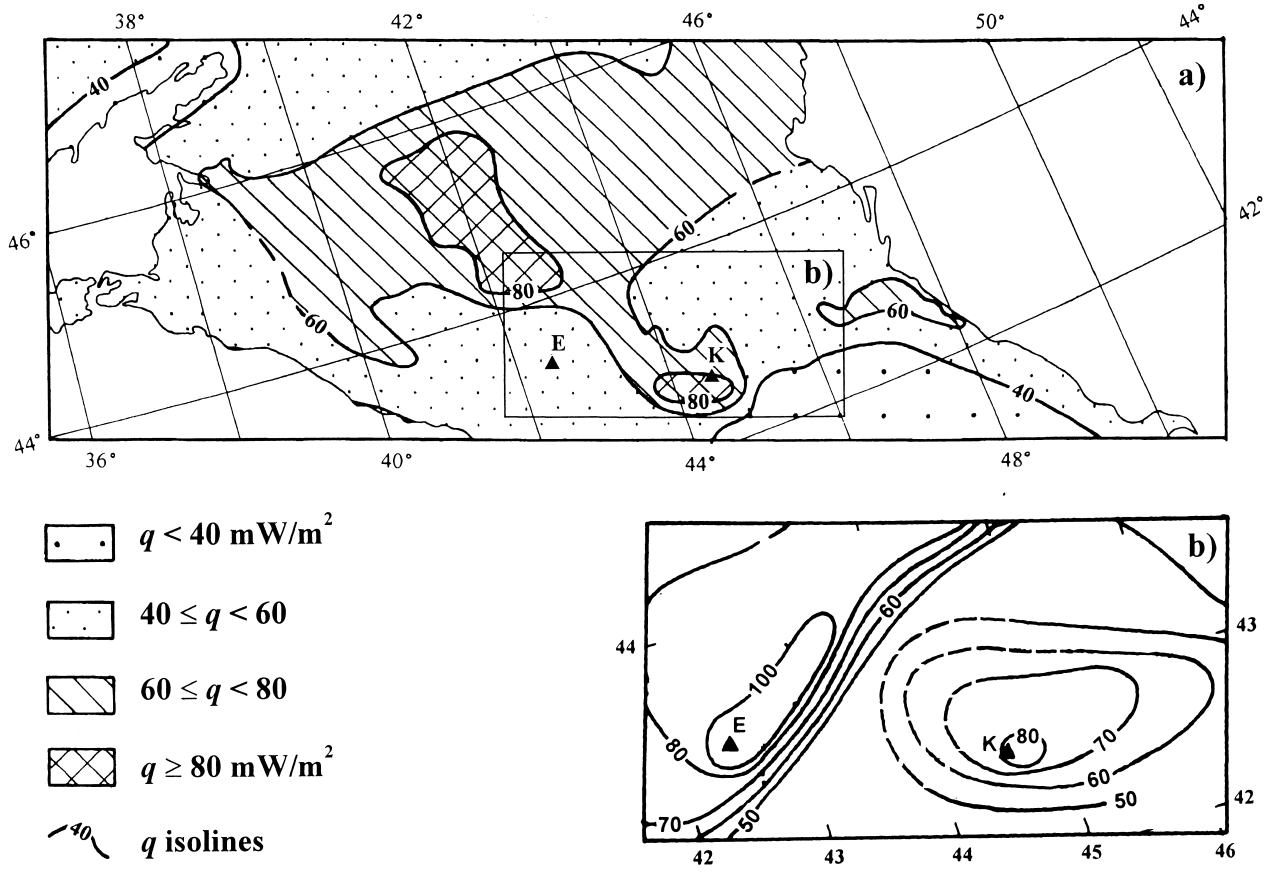

Fig. 8. Lateral variations of heat flow density, q, in the Northern Caucasus. (a) a simplified fragment of the map from (Hurtig, 1992), the rectangle bounds the area shown on (b) presenting a fragment of the q isolines map from (Moisseenko and Negrov, 1993). Abbreviations: (E) Elbrus and (K) Kazbek volcanoes.

comparison of the two available versions of maps (Fig. 8). One of them (Fig. 8b) shows that the Elbrus and the Kazbek positive q anomalies are separated by a narrow band of lower $q < 50$ mW/m^2; this version agrees with the R-value distribution. Regarding the north-western segment, only a few q-values are available and potential q-R relationships remains a subject of future studies.

Synthesis of the R_{av} and q_{av}-values for different parts of the Northern Caucasus (Fig. 9) shows a direct correlation between these parameters. Their coupled minima in the south-eastern segment of the Greater Caucasus and in the Sadon-Uravi zone are particularly remarkable. Helium isotope data demonstrate a close similarity between the Elbrus and Kazbek areas whereas uncertainty in heat flow density distribution seems to result from the lack of geothermal data.

Summarising, the data discussed above supports the concepts proposing transfer of species and thermal energy from the mantle into the crust by silicate melts (Polyak et al., 1979a; Polyak and Tolstikhin, 1985; O'Nions and Oxburgh, 1988).

6. CONCLUSIONS

^{3}He/^{4}He $= R$ in subsurface fluids of the Northern Caucasus vary insignificantly with time and depth and therefore may be used to study patterns produced by lateral variations in R.

Lateral R-variations depend on tectonic-magmatic zoning. The lowest average $R_{av} = (5.36 \pm 0.73) \times 10^{-8}$ characterises the Indol-Kuban and Terek-Caspian foredeeps filled with Alpine molasse. Slightly enhanced $R_{av} = (7.51 \pm 1.08) \times 10^{-8}$ is typical of the epi-Hercynian Scythian plate. In the central part of the plate, R-values are increasing in south-east direction through the Stavropol arch, $(1.6-4.5) \times 10^{-7}$ towards the Caucasus Mineral Waters area (CMW), $R_{av} = (7.6 \pm 0.9) \times 10^{-6}$, and further southward to the central segment of the Greater Caucasus, with the maximum values of $(0.7-0.9) \times 10^{-5}$ near the Elbrus and Kazbek volcanoes.

This tendency implies a correlation between high R-values and proximity to magmatic bodies. Such bodies are indeed observed as laccolithes in the CMW area and form young volcanic centres on the northern slope of the Greater Caucasus. So, the enhanced R are manifested much wider than the Neogene-Quaternary magmatism and reflect degassing of magmatic reservoirs including those yet unknown.

Sr-R inverse isotope correlation emphasises role of silicate melts as carriers of volatile and lithophile mantle species. Direct relationships between averaged R_{av}-values and conductive heat flow densities, q_{av}, indicate that these very melts also transfer mantle heat into the crust. Evolution of the heat sources is recorded by fission-track ages of the pre-Alpine basement within the western segment of the orogene, where R-values decrease with age.

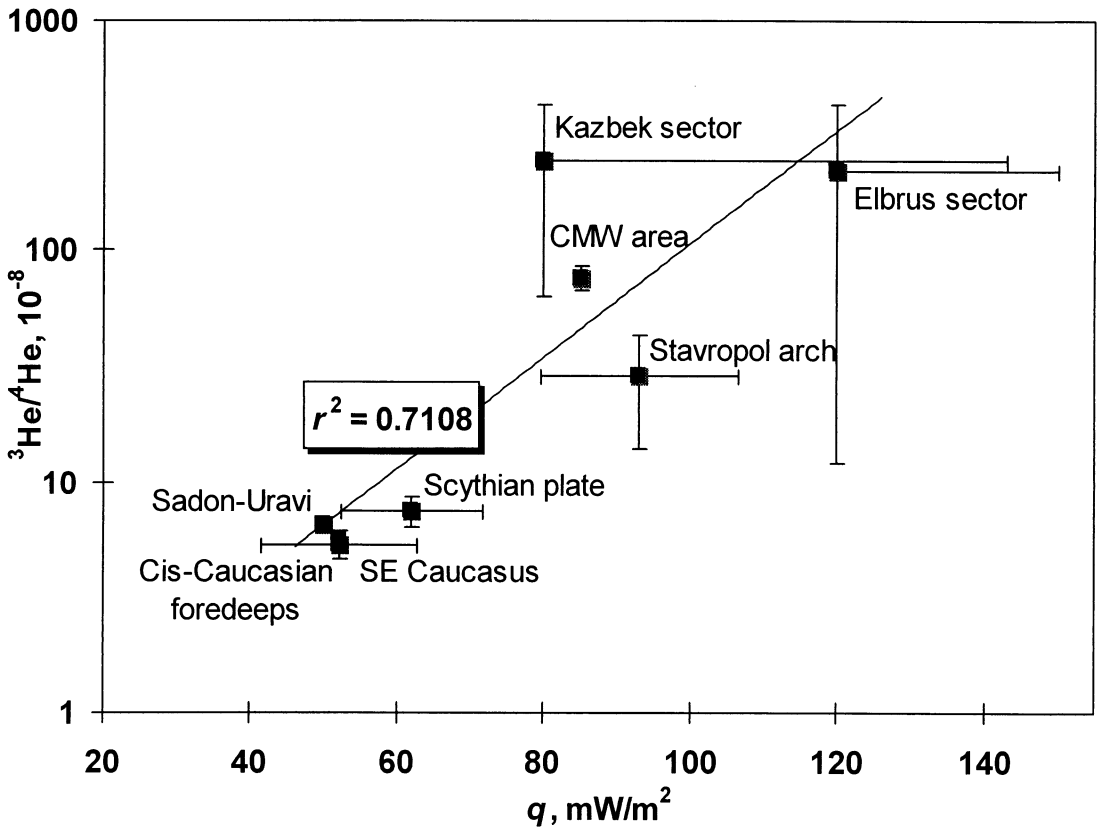

Fig. 9. Relationship between the background conductive heat flow density, q (data from: Smirnov et al., 1992; Moisseenko and Negrov, 1993) and the helium isotope composition in fluids, R, in the Northern Caucasus. Errors are 1 σ (in Sadon-Uravi zone and south-eastern segment of the Greater Caucasus not determined), q errors for Elbrus and Kazbek areas are conventional; the line shows the statistically significant regression (exponential approximation, $r_{R/q} = 0.843 > 0.707 = r_{0.05,\, f = k-2 = 6}$).

Generally CO_2-bearing fluids show elevated $^3He/^4He$ ratios in contrast to CH_4 gases, and a few N_2-rich gases display highly variable ratios. Relationships between the major constituents and noble gas isotopes indicate fractionation, loss, and gain of these species as the processes controlling the compositions of underground fluids.

Acknowledgments—The authors thank R. K. O'Nions for helpful discussions and co-ordination of this study supported by the INTAS Grant 94-3165 and by the Russian Foundation for Basic Researches, Project 96-05-64313. We also express our gratitude to A. G. Gurbanov and S. N. Bubnow for providing unpublished $^{87}Sr/^{86}Sr$ data and discussions. The paper greatly benefited from helpful and constrictive reviews from two anonymous referees; they also considerably improved the language.

REFERENCES

Adamiya Sh. A., Gabuniya G. L., Kuteliya Z. A., Khuzishvili O. D., and Zimakuridze G. K. (1989) Typical tectonic features of the Caucasus. In *Geodynamics of Caucasus* (eds. A. A. Belov and M. A. Satian) pp. 3–15. Moscow, Nauka Publ. (in Russian).

Allard P., Jean-Baptiste Ph., D'Alessandro W, Parello F., Parisi B., and Flehoc C. (1997) Mantle derived helium and carbon in groundwaters and gases of Mount Etna, Italy. *Earth Planet. Sci. Lett.* **148,** 501–516.

Ballentine C. J. and O'Nions R. K. (1993) The use of natural He, Ne and Ar isotopes as constraints on hydrocarbon transport. *Proc. 4th Conf. Petroleum Geology of Northwest Europe* (ed. J. B. Parker, Ed.) pp. 1339–1345. London.

Ballentine C. J. and O'Nions R. K. (1994) The use of natural He, Ne and Ar isotopes to study hydrocarbon-related fluid provenance, migration and mass balance in sedimentary basins. In *Geofluids: Migration and evolution of fluids in sedimentary basins* (ed. J. Parnell), *Geol. Soc. Spec. Publ.* **78,** 347–361.

Ballentine C. J., O'Nions R. K., Oxburgh E. R., Horvath F., and Deak J. (1991) Rare gas constraints of hydrocarbon accumulation, crustal degassing and groundwater flow in the Pannonian Basin. *Earth Planet. Sci. Lett.* **105,** 229–246.

Buachidze G. I. (1979) Temperature distribution in the Earth's crust of the Western Caucasus and the Black Sea. In *Terrestrial heat flow in Europe* (eds. V. Cermak and L. Rybach, Eds.) pp. 316–323. Springer-Verlag Publ.

Buachidze G. I. and Mkheidze B. S. (1989) *Natural gases of Georgia.* Tbilisi, Metsniereba Publ. (in Russian).

Bubnov S. N., Goltsman Yu. V., and Pokrovsky B. G. (1995) Sr, Nd and O isotopic systems as indicators of origin and evolution of primary melts of the recent lavas in the Elbrus volcanic area of the Greater Caucasus. *XIV Symp. on isotope geochemistry* (abstracts), 19–21 Oct. 1995, Moscow, GEOKHI Publ., 28–29 (in Russian).

Chapman D. S. and Pollack H. N. (1976) Global heat flow: New look. *Earth Planet. Sci. Lett.* **28,** 23–32.

Cornides I., Takaoka N., Nagao K., and Matsuo S. (1986) Contribution of mantle derived gases to subsurface gases in a tectonically quiescent area, the Carpathian Basin, Hungary, revealed by noble gas measurements. *Geochim. J.* **20,** 119–125.

Craig H. and Craig V. (1983) Helium isotopes and geochemical studies in Tibet and Eastern China. *EOS* **15,** 549 (abstr.).

Deak J., Horvath F., Martell D. J., O'Nions R. K., Oxburgh E. R., and Stegena L. (1989) Helium isotopes in geothermal waters from northwest Hungary. *AAPG Mem.* **45,** 293–296.

Elliot T., Ballentine C. J., O'Nions R. K., and Ricchiuto T. (1993) Carbon, helium, neon and argon isotopes in a Po Basin (northern Italy) natural gas field. *Chem. Geol.* 106, 429–440.

Farley K. A. (1995) Cenozoic variations in the flux of interplanetary dust recorded by ^{3}He in a deep-sea sediment. *Nature* **76,** 153–156.

Faure G. and Powell J. L. (1972) Strontium Isotope Geology. Berlin, Springer-Verlag.

Garetovskaya I. V., Krasnopevtseva G. V., Sizov A. V., Faitelson A. Sh., and Shchukin Yu. K. (1986) Seismic and gravimetric study of the North Caucasus seismic-dangerous zone (Caucasus Mineral waters and Elbrus area). In *Main problems of seismotectonics* (ed. Yu. K. Shchukin) pp. 105–119. Moscow, Nauka Publ. (in Russian).

Gazaliev I. M. and Prasolov E. M. (1988) On the origin of the Daghestan gas issues from isotopic data. *Doklady AN SSSR* **298,** 1218–1221 (in Russian).

Gemp S. D., Lagunova I. A., and Nesmelova Z. N. (1979) Genetic features of mud volcano gases. *Geokhimiya* **12,** 1859–1867 (in Russian).

Giggenbach W. F., Confiantini R., Jangi B. L., and Truesdell A. H. (1983) Isotopic and chemical composition of Parbati valley geothermal discharge, North-West Himalayas, India. *Geothermics* **12,** 199–222.

Griesshaber E., O'Nions R. K., and Oxburgh E. R. (1989) Helium isotope systematics in crustal fluids from West Germany and adjacent areas. In *European Geothermal Update* (eds. K. Louwrier, E. Staroste, J. D. Garnish, and V. Karkoulias) pp. 407–418. Kluwer Acad. Publ.

Hill R. I., O'Nions R. K., Oxburgh E. R., and Hooker P. J. (1986) Assessment of deep volatile fluxes by helium isotope ratios. *British Geol. Surv. Rept.* FLPU **86–2,** Keyworth, England, 80–97.

Hooker P. J., Bertrami P. J., Lombardi S., O'Nions R. K., and Oxburgh E. R. (1985) Helium-3 anomalies and crust-mantle interaction in Italy. *Geochim. Cosmochim. Acta* **49,** 2505–2513.

Hurtig E., Editor-in-Chief (1992) Geothermal Atlas of Europe. Hermann Haak Verlaggeselschaft mbH, Geoforschungs Zentrum Potsdam.

Ivanov D. A., Bubnov S. N., Volkova V. M., Goltsman Yu. V., Zhuravlev D. Z., and Bairova Zh. D. (1993) Sr and Nd isotopic composition in Quaternary lavas of the Greater Caucasus in relation to problem of their origin. *Geokhimiya* **3,** 342–353 (in Russian).

Ivanov Val. V., Editor-in-Chief (1972) Caucasian Mineral Waters. *Proc. TsNIIKiPh, vol. XXI. The USSR Ministry of Health Service Publ.* (in Russian).

Ivanov Vas. V., Medovyi V. I., and Dobrovolskaya V. I. (1978) Fields of helium concentrations in the sedimentary sequences. *Sovetskaya Geologiya* **2,** 48–63 (in Russian).

Kamensky I. L., Tolstikhin I. N., and Vetrin V. R. (1990) Juvenile helium in ancient rocks: I. ^{3}He excess in amphiboles from 2.8 Ga charnockite series: Crust-mantle fluid in intracrustal magmatic processes. *Geochim. Cosmochim. Acta* **54,** 3115–3122.

Kipfer R. (1991) Primordial Edelsgase als Tracer fuŕ Fluide aus dem Mantel. D. Sci. dissertation no. 9463, Eidgenössischen Technischen Hochschule Zürich.

Koronovsky N. V. (1994) Geodynamic situations of the Late Cenozoic volcanism manifestations in the Aegean, Anatolian and Caucasian regions (central part of the Alpine fold belt)). *Vestnik Moskovskogo Universiteta ser. 4 (geol.)* **1,** 35–48 (in Russian).

Kral J. and Gurbanov A. G. (1996) Apatite fission track data from the Greater Caucasus pre-Alpine basement. *Chem. Erde* **56,** 177–192.

Kutas R. I. (1993) Thermal field and geothermal regime of lithosphere. In *Lithosphere of Central and Eastern Europe: Generalisation of research data* (ed. A. V. Chekunov) Chap. 6, pp. 114–135. Kiev, Naukova Dumka Publ. (in Russian).

Lagunova I. A. (1974) On the CO_2 genesis in mud volcano gases of the Kerch'-Taman' region. *Geokhimiya* **6,** 721–730 (in Russian).

Lavrushin V. Yu., Polyak B. G., Prasolov E. M., and Kamensky I. L. (1996) Sources of substance in mud volcanism products. *Lithol. Min. Res.* **6,** 625–647 (in Russian).

Loosli H. H., Lehman B. E., Gautschi A., and Tolstikhin I. N. (1995) Helium isotopes in rocks, minerals, and related groundwaters. In *Proc. 8th Int. Symp Water-Rock Interaction* (eds. Y. K. Kharaka and O. V. Chudaev). pp. 31–34. Balkema, Rotterdam.

Mamyrin B. A. and Tolstikhin I. N. (1984). Helium isotopes in nature. Elsevier, Amsterdam.

Marcantonio F., Higgins S., Anderson R. F., Stute M., Schlosser P., Rasbury E. T. (1998) Terrigenous helium in deep sediments. *Geochim. Cosmochim. Acta* **62,** 1535–1543.

Martell D. J., Deak J. N., Doveni P., Horvath F., O'Nions R. K., Oxburgh E. R., Stegena L., and Stute M. (1989). The leakage rate of mantle helium in the Pannonian Basin. *Nature* **342,** 908–912.

Marty B., O'Nions R. K., Oxburgh E. R., Martell D., and Lombardi S. (1992) Helium isotopes in Alpine regions. *Tectonophysics* **206,** 71–78.

Marty B., Torgersen T., and Meynier V. (1993) Helium isotopes fluxes and groundwater ages in the Dogger aquifer, Paris Basin. *Water Res. Res.* **29,** 1025–1035.

Marty B., Trull T., Lussiez P., Basile I., and Tangui J.-C., (1994) He, Ar, O, Sr and Nd isotope constraints and evolution of Mount Etna magmatism. *Earth Planet. Sci. Lett.* **126,** 23–39.

Marty B. and Tolstikhin I. N. (1998) CO_2 fluxes from mid-ocean ridges, arcs and plumes. *Chem. Geol.* **145,** 233–248.

Matthews A., Fouillac C., Hill R., O'Nions R. K., and Oxburgh E. R. (1987) Mantle-derived volatiles in continental crust: The Massif Central of France. Earth Planet. Sci. Lett. **85,** 117–128.

Matveeva E. S., Tolstikhin I. N., and Yakutseni V. P. (1978) Helium-isotope criterion for gases origin and revealing the neotektogenesis zones (on the example of Caucasus)). *Geokhimiya* **3,** 307–317 (in Russian).

Merrihue C. (1964) Rare gas evidence for cosmic dust in modern Pacific red clay. *Ann. New York Acad. Sci.* **119,** 351–367.

Milanovsky E. E. and Koronovsky N. V. (1973) Orogenic volcanism and tectonics of the Alpine belt of Eurasia. Moscow, Nedra Publ. (in Russian).

Milanovsky E. E., Rastsvetaev L. M., Kukhmazov S. U., Birman A. S., Kurdin N. N., Simako B. G., and Tveritinova T. Yu. (1989) Newest geodynamics of the Elbrus-Mineral Waters region in Northern Caucasus. In *Geodynamics of Caucasus* (eds. A. A. Belov and M. A. Satian). Moscow, Nauka Publ. (in Russian).

Moisseenko U. I. and Negrov O. B. (1993) Geothermal conditions of the North-Caucasus seismic-dangerous zone. In *Geothermics of seismic and non-seismic zones* (eds. V. I. Kononov, F. N. Yudakhin, and V. B. Svalova). pp. 32–40. Moscow, Nauka Publ. (in Russian).

Nagao K. (1979) Isotopic composition of terrestrial rare gases and application to earth science. Ph. D. dissertation, Osaka University.

Nuti S., (1984) Elementary and isotopic compositions of noble gases in geothermal fluids of Tuscany, Italy. *Geothermics* **13/3,** 215–226.

O'Nions R. K. and Ballentine C. J. (1993). Rare gas studies on basin scale fluid movement. *Phil. Trans. R. Soc. Lon. A* **344,** 141–156.

O'Nions R. K. and Oxburgh E. R. (1988) Helium, volatile fluxes and the development of continental crust. *Earth Planet. Sci. Lett.* **90,** 331–347.

Oxburgh E. R., O'Nions R. K., and Griesshaber E. (1987) ^{3}He/^{4}He measurements in Greece and southern Germany. In *CEC Proc. Contractors' Meeting/Workshop Geochem. Toulouse, 24–25 Nov.* (ed. K. Lowrier and J. Garnish), 183–190.

Oxburgh E. R., O'Nions R. K., and Hill R. I. (1986) Helium isotopes in sedimentary basins. *Nature* **324,** 632–635.

Philip H., Cisternas A., Gvishiani A., and Gorshkov A. (1989) The Caucasus: An actual example of the initial stages of continental collision. *Tectonophysics* **161,** 1–21.

Pohl I. R., Hess J. S., Kober B., and Borsuk A. M. (1993) Origin and petrogenesis of Miocene trachyrhyolites (A-type) from the Greater Caucasus northern part. In *Magmatism of rifts and folded belts* pp. 109–124. Moscow, Nauka Publ. (in Russian).

Polyak B. G. (1988) Heat-mass flux from the mantle in the main tectonic units of the earth crust. Moscow, Nauka Publ. (in Russian).

Polyak B. G. and Smirnov Ya. B. (1968) Relation of terrestrial heat flow to tectonic structure of continents. *Geotektonika* **4,** 3–19 (in Russian).

Polyak B. G. and Tolstikhin I. N. (1985) Isotopic composition of the Earth's helium and the motive forces of tectogenesis. *Chem. geol.* **52,** 9–33.

Polyak B. G., Tolstikhin I. N., and Yakutseni V. P. (1979a) Isotopic

composition of helium and terrestrial heat flow: Geochemical and geophysical aspects of tectogenesis. *Geotektonika* **5,** 3–23 (in Russian).

Polyak B. G., Prasolov E. M., Buachidze G. I., Kononov V. I., Mamyrin B. A., Surovtseva L. I., Khabarin L. V., and Yudenich V. S. (1979b) Isotopic composition of He and Ar in fluids of the Alps-Apennines region and its relation to volcanism. *Doklady AN SSSR* **247,** 1220–1225 (in Russian).

Polyak B. G., Prasolov E. M., Kononov V. I., Verkhovskiy A. B., Gonzalez A., Templos L. A., Espindola J. M., Arellano J. M., and Manon A. (1982) Isotopic composition and concentration of inert gases in Mexican hydrothermal systems. *Geofisica Int.* **21,** 193–227.

Polyak B. G., Prasolov E. M., Tolstikhin I. N., Kozlovtseva S. V., Kononov V. I., and Khutorskoi M. D. (1992) Helium isotopes in fluids of the Baikalian Rift zone. *Izvestiya AN SSSR, ser. geol.,* **10,** 18–33 (in Russian).

Polyak B. G., Khutorskoi M. D., Kamensky I. L., and Prasolov E. M. (1994) Heat-mass flux from the mantle in Mongolia (on the base of helium isotopes and geothermal data)) *Geokhimiya* **12,** 1693–1706 (in Russian).

Popov V. S. (1987) Geochemistry of the recent Caucasus volcanic rocks and their origin. In *Geochemistry of continental volcanism* (ed. S. V. Grigoryan), Chap. 5, pp. 143–238. Moscow, Nauka Publ. (in Russian).

Potapov E. G., Voitov G. I., Korobeinik G. S., Miller Yu. M., and Yakovleva V. P. (1998) The features of spontaneous gases and carbon isotope composition of Zheleznovodsk mineral water deposit. *Doklady AN SSSR* **359,** 106–108 (in Russian).

Prasolov E. M. (1990) Isotope geochemistry and origin of natural gases. Leningrad, Nedra Publ. (in Russian).

Sano Y., Wakita H., Italiano F., and Nuccio M. P. (1989) Helium isotopes and tectonics in Southern Italy. *Geophys. Res. Lett.* **16,** 511–514.

Sclater J. G. and Francheteau J. (1970) The implication of terrestrial heat flow observations on current tectonic and geochemical models of the crust and upper mantle of the earth. *Geophys. Roy. Astron. Soc.* **20,** 509–542.

Sclater J., Parsons B., and Jaupart C. (1981) Oceans and continents: Similarities and differences in mechanism of heat flow. *J. Geophys. Res.* **86,** 11535–11552.

Shengelaya G. Sh. (1978) 3-d gravitation model of deep structure of the Caucasus earth crust. *Sovetskaya geologiya* **12,** 102–107 (in Russian).

Shcherbak V. P. and Gurevich N. G. (1971) Some geochemical peculiarities of gases in the Caucasian Mineral Waters, CMW. *Proc. TsNIIKiPh,* vol. 33, *The USSR Ministry of Health Service Publ.,* 119–124 (in Russian).

Smirnov Ya. B., Kutas R. I., and Zui V. I. (1992) USSR. In *Geothermal Atlas of Europe* (ed. E. Hurtig), pp. 91–101. Explanatory text, Hermann Haak Verlaggeselschaft mbH Geoforschungs Zentrum Potsdam.

Stute M., Sonntag C., Deak J., and Schlosser P. (1992) Helium in deep circulating groundwater in the Great Hungarian Plain: Flow dynamics and mantle helium fluxes. *Geochim. Cosmochim. Acta* **56,** 2051–2067.

Tedesco D. (1996) Chemical and isotopic investigations of fumarolic gases from Ischia island (southern Italy): Evidences of magmatic and crustal contribution. *J. Volcanol. Geotherm. Res.* **74,** 233–242.

Tedesco D., Nagao K. (1996) Radiogenic 4He, 21Ne and 40Ar in fumarolic gases on Volcano: Implication for the presence of continental crust deneath the island. *Earth Planet. Sci. Lett.* **144,** 517–528.

Tedesco D., Nagao K., and Scarci P. (1998) Noble gas isotopic ratios from historical lavas and fumaroles ar Mount Vesuvius (southern Italy): Constraints for current and future volcanic activity. *Earth Planet. Sci. Lett.* **164,** 61–78.

Tedesco D., Allard P., Sano Y., Wakita H., and Pece R. (1990) Helium-3 in subaerial and submarine fumaroles of Campi Flegrei caldera, Italy. *Geochim. Cosmochim. Acta* **54,** 1105–1116.

Tolstikhin I. N., Lehmann B. E., Loosli H. H., and Gautschi A. (1996) Helium and argon isotopes in rocks, minerals, and related groundwaters: A case study in northern Switzerland. *Geochim. Cosmochim. Acta* **60,** 1497–1514.

Tolstikhin I. N., Lehmann B. E., Loosli H. H., Kamensky I. L., Nivin V. A., Orlov S. P., Ploschansky L. M., Tokarev I. V., and Gannibal M. A. (1999) Radiogenic helium isotope fractionation: The role of tritium as ^{3}He precusor and geochemical implications. *Geochim. Cosmochim. Acta* **63,** 1605–1611.

Trull T., Nadeau S., Pineau F., Polve M., and Javoy M. (1993) C-He systematics in hotspot xenoliths: Implications for mantle carbon contents and carbon recycling. *Earth Planet. Sci. Lett.* **118,** 43–64.

Trebukhova T. M. and Chesalov S. M. (1990) Distribution and formation regularities for mineral waters in the Zheleznovodsk zone. *Proc. Sci. Res. Inst. for Phys. Methods of Rehabilitation. Moscow,* 5–66 (in Russian).

Voitov G. I., Gazaliev I. M., and Shapazov I. M. (1984) The ^{40}Ar/^{36}Ar ratio in gas issues of the South Daghestan and Daghestan tectonic wedge). *Doklady AN SSSR* **276,** 464–468 (in Russian).

Voitov G. I., Korobeinik G. S., Miller Yu. M., Potapov E. G., and Yakovleva V. P. (1998) Chemical features and fluctuations in isotopic composition of carbon from spontaneous gases of Piatigorsk mineral water deposit. *Doklady AN SSSR* **359,** 540–542 (in Russian).

Voitov G. I., Miller Yu. M., Murogova R. N., Potapov E. G., and Yakovleva V. P. (1996) On the isotopic composition of the CO_2 carbon from spontaneous gases of Kislovodsk mineral water deposit. *Doklady AN SSSR* **350,** 681–683 (in Russian).

Voitov G. I., Miller Yu. M., Murogova R. N., Potapov E. G., and Rudakov V. P. (1994) On the chemical and C-isotopic fluctuations of spontaneous gases from Naguty mineral water deposit. *Doklady AN SSSR* **339,** 666–669 (in Russian).

Voitov G. I., Korobeinik G. S., Miller Yu. M., Potapov E. G., and Rudakov V. P. (1993) New data on C-isotopic composition for spontaneous gases from Caucasian Mineral Waters. *Doklady AN SSSR* **333,** 380–384 (in Russian).

Yakovlev L. E. and Polyak B. G. (1998) The origin of a helium isotope anomaly in the north of the Mount Elbrus Region. *Vulkanol. Seismol.* **19,** 769–783.

Yokoyama T., Nakai S. and Wakita H. (1999) Helium and carbon isotopic composition of hot spring gases in the Tibetan Plateau. *J. Volcanol. Geotherm. Res.* **88,** 99–107.

Zor'kin L. M., Krylova T. A., Bunakova G. V., and Slastenko L. G. (1981) On the carbon isotope composition from organic matter, rocks, water and spontaneous gas of Caucasian Mineral Waters. *Doklady AN SSSR* **257/3,** 711–713 (in Russian).

Zuhuang C., Huxin S., Songlin M., Guangwei L., and Xizhong S. (1986) Isotopic study on depth of the recent activities of Yangbajing section of the fault in front of Nianquing Tanggula Mountains. *Kexue Tongbao* **30,** 1401–1405.